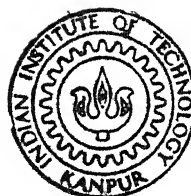# EXPERIMENTAL INVESTIGATIONS INTO THE SPIKE PROFILE OBTAINED DURING ELECTROCHEMICAL DRILLING
OF
BLIND HOLES

By

P. S. SREEJITH

DEPARTMENT OF MECHANICAL ENGINEERING
INDIAN INSTITUTE OF TECHNOLOGY KANPUR
JANUARY, 1992

EXPERIMENTAL INVESTIGATIONS INTO THE SPIKE PROFILE OBTAINED DURING ELECTROCHEMICAL DRILLING

OF
BLIND HOLES

A Thesis Submitted

In Partial Fulfilment of the Requirements

for the Degree of

MASTER OF TECHNOLOGY

by

P.S. SREEJITH

to the

DEPARTMENT OF MECHANICAL ENGINEERING

INDIAN INSTITUTE OF TECHNOLOGY KANPUR
JANUARY, 1992

CERTIFICATE

16/1/92

This is to certify that the work entitled, "Experimental Investigations into the Spike Profile Obtained During Electrochemical Drilling of Blind Holes" submitted by P. S. Sreejith has been carried out under our guidance and has not been submitted elsewhere for a degree.

Dr. V. K. Jain   Dr. G. K. Lal
Professor,   Professor.
Dept. of Mech. Engg.,   Dept. of Mech. Engg.,
IIT, Kanpur   IIT, Kanpur

TO

MY WIFE BEENA

AND

DAUGHTER SREEVARSHA

ACKNOWLEDGEMENTS

I am extremely grateful to my thesis Supervisors. Dr. V. K. Jain and Dr. G. K. Lal for their valuable guidance throughout the present work.

A special debt of gratitude is also due to my friend Mr. Philip Koshy, Ph.D. student for his timely advice. encouragement and assistance throught my studies here.

My regards to Mr. Raghuram. Research Engineer, for his suggestions and co-operation during this work.

I am thankful to the staff of Manufacturing Science Laboratory for their help during the project work.

Finally I express my gratitude to all my friends, who made moments at IIT-K memorable and great.

-Sreejith.

CONTENTS

LIST OF FIGURES

LIST OF TABLES

NOMENCLATURE

A	Atomic Weight, Kgs
b_a	Regression Coefficient
f	Feed rate, mm/s
G	Grand total of the responses
I	Current, A
k	Number of variables
m	Mass, Kgs
N	Number of Experiments
n_1	Number of repetitive experiments
n_2	Number of non repetitive experiments
x_i	Coded value of variables
y_n	Response
$\bar{y}_a$	Mean of the responses of the central points
y_{an}	Response of Central Point
y_n	Mean of all the responses
z	Valency
μ	Micro-meter
ECM	Electrochemical Machining
ECD	Electrochemical Drilling
RSM	Response Surface Methodology
SEM	Scanning Electron Microscope
IGA	Inter Granular Attack

ABSTRACT

The Electrochemical Machining (ECM) has in recent times, emerged as an important advanced machining process. In spite of its wide applications it has not been possible to solve the different problems associated with the process. Thus its full capabilities have not been utilized. Electrochemical drilling (ECD) is perhaps the simplest electrochemical machining process because the tool most commonly used consists only of a metal tube with insulation on the outer wall. It has been applied successfully to several practical applications in industries to get circular and non-circular holes. There have been many attempts to calculate the anode profile produced during electrochemical machining, but hardly any attempt has been made to predict the spike profile produced during drilling of blind holes by ECM. Also, very limited experimental data are available about the spike profile obtained during ECD of blind holes in difficult to machine materials.

In the present work, an experimental study of the spike produced at the stagnation zone of blind holes is made. It consists of an experimental programme to study the effects of various parameters on the characteristics of the spike formed during ECD. Experiments have been planned based on the statistical response surface methodology (RSM). Regression equations correlating the process parameters to the responses are obtained. An attempt also has been made to optimize the process

conditions to minimize the spike volume. From the study it is seen that the variables like the diameter of the hole drilled at the centre of the tool for electrolyte flow, the taper angle of the hole, voltage applied across the tool and workpiece and the feed rate play a major role in determining the characteristics of the spike. The second order polynomial model developed from the experiments adequately represents the relationship between the above said electrochemical drilling parameters. The depth of correlation obtained between the actual values and the values given by the postulated model are satisfactory.

CHAPTER 1

INTRODUCTION AND LITERATURE SURVEY

The mechanical cutting action that arises when a sharp tool makes contact with the workpiece of softer material has been the basis of established machine tool technology for almost two centuries. Indeed the principle on which these machines work continue to be the subject of many investigations. In recent years (2-3 decades) however, attention has turned towards the application of advanced methods of material removal [1]. The different nonconventional machining processes can be broadly classified into the following four classes.

(1) Mechanical processes which include ultrasonic machining, abrasive jet machining, water jet cutting. abrasive flow machining etc.

(2) Thermal processes like electrical discharge machining, laser beam machining, plasma are cutting, electron beam machining etc.

(3) Chemical processes like chemical cutting, milling, blanking etc.

(4) Electrochemical processes like electrochemical machining, grinding, deburring, drilling, honing etc.

1.1 Working of Electrochemical Machining process:

Electrochemical machining (ECM) is a process that relies on the principle of electrolysis for material removal. A deplating action between a conductive workpiece and a shaped tool produces a predictable erosion of the workpiece. In this process, a high

current, low voltage D. C. power supply source is connected between an electrically conductive tool and workpiece. As shown in Fig. 1.1 the shaped tool is connected to the negative polarity and the workpiece is connected to the positive. A conductive electrolyte flows through a small inter electrode gap (IEG) between the tool and the workpiece, thus providing the necessary path for the electric current to flow. If conditions are chosen correctly, dissolution of the anode (workpiece) occurs. The shaped tool concentrates the electric current on those parts of the workpiece for which preferential removal of metal is required. Means are provided to advance the tool (cathode) at a steady speed towards the workpiece, and the machine must be stopped when the tool has advanced far enough. Then the surface of the workpiece should be bright and smooth and shaped similarly to the surface of the tool. The removal of metal from the anode is a smooth, gentle process, in complete contrast to the ploughing or smearing action of conventional machining processes [2].

Electrochemical machining process is quite often employed when shaped cavities are to be machined into alloys that are difficult to shape by conventional methods. These cavities are quickly produced by ECM by simply feeding the tool into the workpiece until the required depth is reached.

1.2 Technology of the process:

ECM is similar to electropolishing in that it also is an anode dissolution process. But the rates of metal re oval offered by the polishing process is considerably less than those needed in metal machining practice. To illustrate how ECM meets these requirements and moreover, how it is used to shape metals, the

electrolysis arising from iron in aqueous sodium chloride is considered [3].

When a potential difference is applied across the electrodes, several possible reactions can occur at the anode and the cathode. Certain reactions, however are more likely to arise than others. Thus preferences can be explained in terms of the energy that is available for each reaction. In the present example, the probable anodic reaction is dissolution of iron,

$$Fe \longrightarrow Fe^{++} + 2e \qquad (1.1)$$

At the cathode the reaction is likely to be the generation of hydrogen gas and the production of hydroxyl ions,

$$2H_2O + 2e \longrightarrow H_2\uparrow + 2OH^- \qquad (1.2)$$
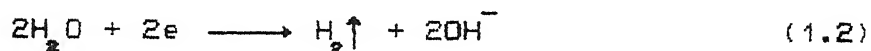
The outcome of these electrochemical reactions is that the metal ions combine with the hydroxyl ions to precipitate out as ferrous hydroxide i.e.,

$$Fe + 2H_2O \longrightarrow Fe(OH)_2 + H_2\uparrow \qquad (1.3)$$
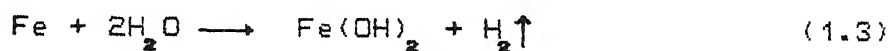
Ferrous hydroxide may react further with water and oxygen to form ferric hydroxide.

$$4Fe(OH)_2 + 2H_2O + O_2 \longrightarrow 4Fe(OH)_3 \qquad (1.4)$$
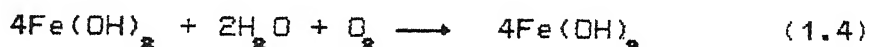
The present electrolysis results in the dissolution of iron from the anode, and the generation of hydrogen at the cathode.

Certain observations relevant to ECM can be made at this stage.

1. Since the anode metal dissolves electrochemically, its rate of dissolution depends, by Faraday's laws of electrolysis, only upon its atomic weight A, its valency z, the current I which is passed, and the time t for which the current passes. The dissolution rate is not influenced by the hardness or other

characteristics of the metal.

2. Since only hydrogen gas is evolved at the cathode, the shape of that electrode remains unaltered during the electrolysis.

The cathode (tool) is usually made of some electrically conducting material such as copper or brass, although special purpose materials like stainless steel which can resist serious dissolution in the electrolyte, which in turn may be an acid or salt solution, are used. No chips appear as in ordinary machining, but only salts or hydroxides of the elemental metals in the workpiece, which are pumped round the electrolyte. These have to be taken out by filtering, chemical precipitation, or as 'sludge'. This purification, either continuous or intermittent, is essential to maintain steady machining conditions. Water must also be added to the solution to replace that consumed by the electrolysis. Plastic tanks and pipe work are used to combat general corrosion of the equipment itself [4].

Electrochemical drilling is a popular way of using ECM. As indicated in Fig. 1.2 a tubular electrode is used as the cathode tool. Electrolyte is pumped down the central bore of the tool, and out through the side gap formed between the wall of the tool and the hole being drilled in the workpiece. The main machining action is carried out in the interelectrode gap formed between the leading edge of the drill-tool and the base of the hole in the workpiece. ECM also proceeds laterally between the side walls of the tool and the component. Since the lateral gap width is larger than that at the leading edge of the tool the machining rate in the sides is much lower. The overall effect of the side ECM is to increase the diameter of the hole that is produced. A wide range

in hole sizes can be drilled, diameters as small as 0.05mm to as large as 20mm have been reported.

Under ideal conditions ECM is capable of producing tolerances of approximately ± 0.012mm, although in daily production the number is closer to ± 0.05mm. The typical overcut at the side of tools is approximately 0.12mm. Surface finish is dependent on the workpiece material, the type of tool used, the electrolyte flow, and the current density. Usually the surface finish at the tip of an ECM tool will be 0.1-0.15μ. The side of the tools may produce surface finishes as rough as 5μ because of low current density [2].

Using hollow tubing as the ECM tool holes as small as 0.76mm in diameter can be drilled. Length/diameter ratios upto 20:1 can be accomplished.

No detrimental effects on materials have been found with ECM when parameters are properly selected. However improper selection of the electrolyte or operating at a current density that is too low can lead to intergranular attack (IGA). This condition results when the process dissolves grain boundaries before the actual metal grains. If undetected, IGA could cause a premature fatigue failure of the part.

Electrochemical drilling is particularly used for producing deep small diameter holes in tough and hard materials. It is extensively used for drilling the cooling holes in gas turbine blades and for many other jobs in the manufacture of gas turbine engines. Shaped holes without burrs can be pierced in thin workpieces, and the process has proved of value in the electronics industry for cutting thin sheets of silicon or germanium.

1.3 Previous Work:

Little literature appears to be available till date, about the profile of the spike that is formed in ECD of blind holes. Larsson and Muzaffaruddin [5] assumed radial current density distribution to determine the spike height. The purpose of their analysis was to show how the shaping performance of electrolyte is related to their electrochemical properties. They used the spike height as an index to demonstrate the effect of solution properties on its shaping performance rather than to predict the actual spike profile. The use of a simple tubular drill with an uninsulated bore constituted a very sensitive test for shaping performance, as the height of the spike produced at the bottom of a blind hole is shown to be dependent on both polarization and current efficiency. They showed that the development of a current density dependent voltage at the electrode-electrolyte interface, and efficiency of an electrolyte are far from negligible in determining the shaping performance of an electrolyte. This is particularly so when machining is in generating mode where there is a wide range of current density. They concluded that polarization plays an important role in reducing the shaping performance of an electrolyte and should not be ignored in any method used to predict workshapes. Here, the assumptions made are far reaching, since the current distribution at the top of the spike will certainly be not radial. Also, the change in electrolyte conductivity due to heating effects and the development of gas bubbles in the electrolyte has not been taken into account.

Kanetkar [6] had suggested a theoretical model for determination of the shape of the tool specifically accounting for the effects of stray current zone to produce the required work shape, while machining under specified conditions. This method accounts for the variation in different process parameters. Tools have been designed for producing profiles obtained experimentally. Design of the electrolyte supply hole in the cathode has been aimed to minimize the spike dimensions, especially the height. This is a case similar to the tool design for external shaping by ECM process. He has also given a complete classification of the different zones obtained in ECD as shown in Fig. 1.3. Fig 1.4 shows the designed tool for obtaining the desired spike profile. In his work the spike profile has been chosen such that it is similar in nature to the spike profile obtained by experimental tool, but lesser in height. Since no experimental results are available about the spike profile in the stagnation zone, the analytically predicted anode profile in that zone has not been compared. The deviation between the analytical and experimental tool shape is because of the following reasons.

1. No consideration for the effect of void fraction in conductivity. Conductivity has been assumed to be a function of temperature alone.

2. Use of simple triangular elements in finite element discretization of the stagnation zone which may not fit exactly with the work or tool boundary, leading to an error.

1.4 Present Work:

From the above literature available it appears that no attempt has been made to find out the profile of the spike that is

formed in the stagnation zone during ECD of blind holes. For a comprehensive and meaningful analysis of anode shape prediction during ECD the analysis of stagnation zone is very important. The work embodied in this thesis has been aimed to find out the actual spike profile during ECD.

The workpiece shape obtained during ECD of blind holes with outward mode of electrolyte flow is shown in Fig. 1.2. It can be seen from the figure that the bottom surface of the hole is not flat instead there will be an unmachined spike formed because of the absence of metal at the hole. Spikes are undesirable features obtained often in blind hole drilling.

Experiments have been planned using the concept of statistical "design of experiments" technique. Four parameters are chosen viz the diameter of the tool hole for the electrolyte flow, taper angle of the hole, voltage applied and feed rate. A 4 factor, 5 level experimental design has been used. Since the main objective is to minimize the spike volume in general and spike height and width in particular, the responses measured were the volume of the spike, its height and width, and an experimental model has been developed.
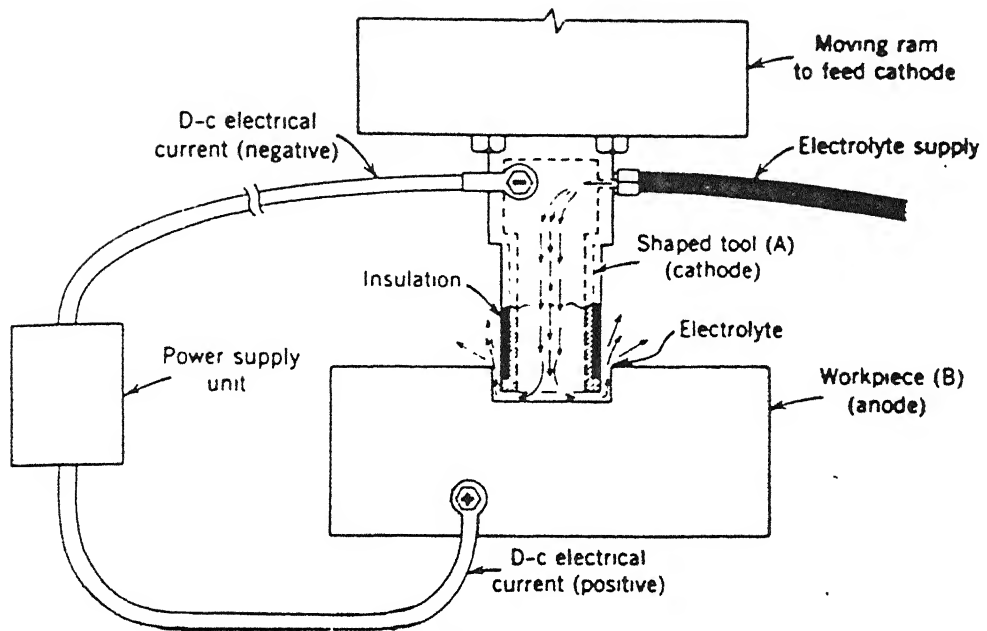
Fig. 1.1 The Electrochemical Machining Process [2]
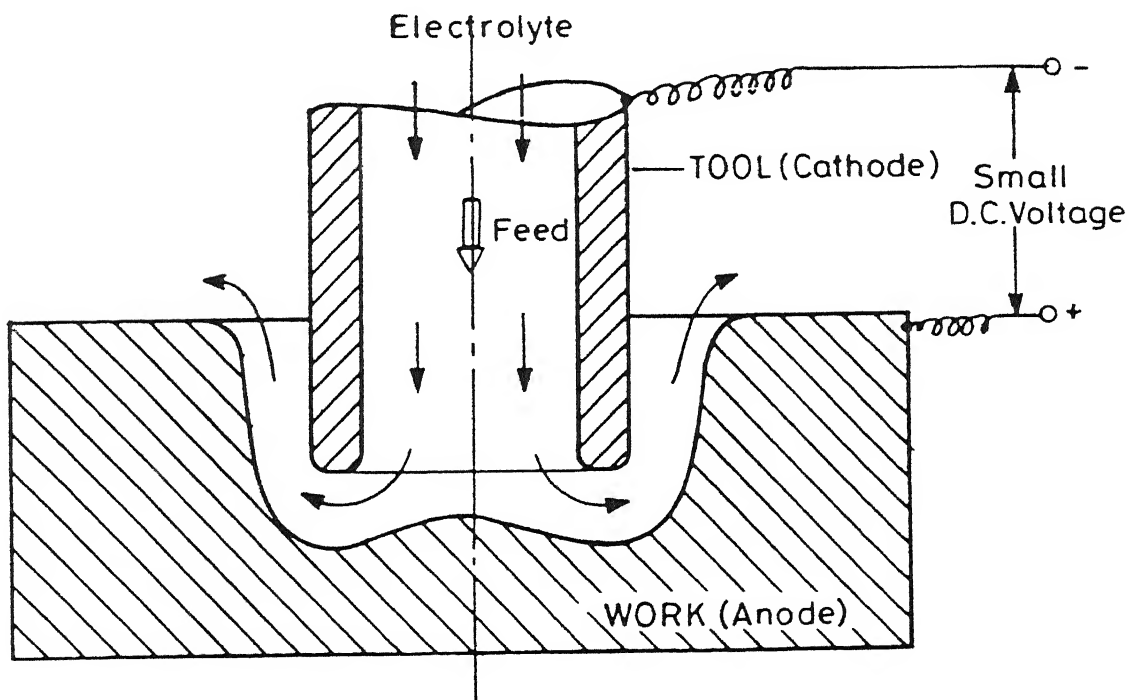

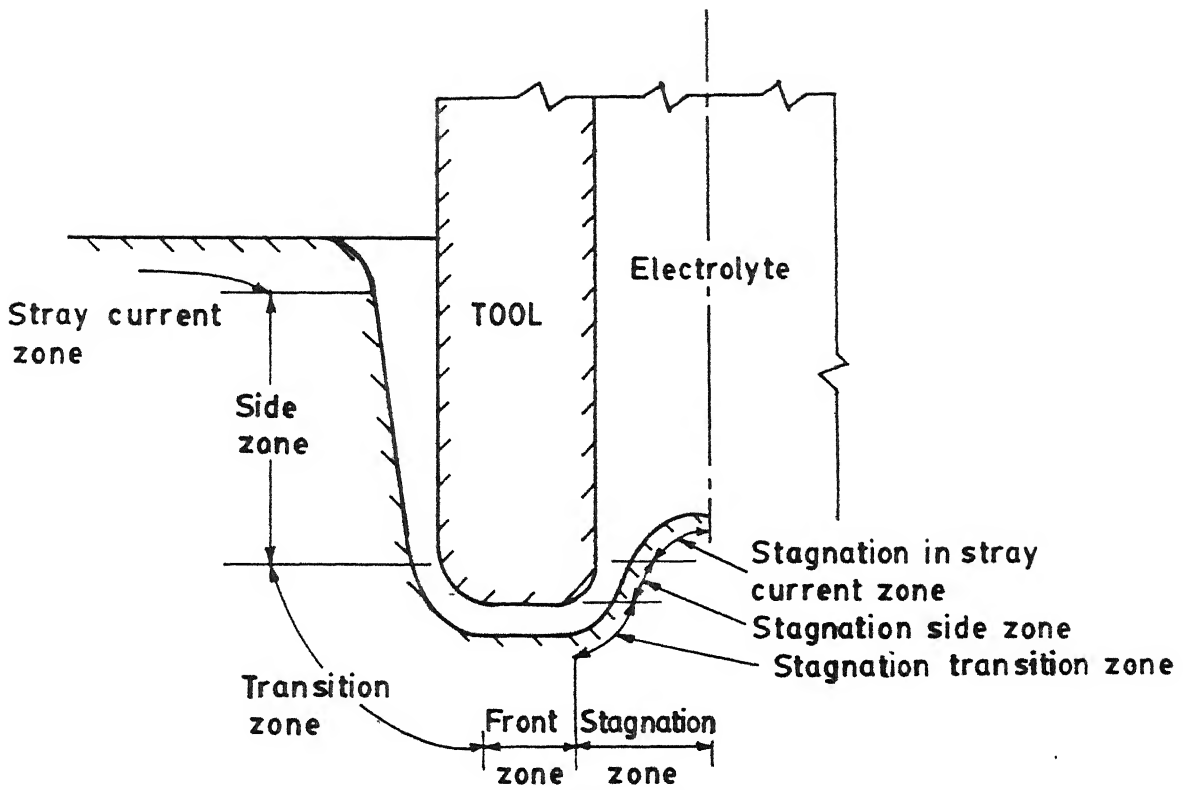**Fig. 1.2 Schematic Diagram of ECD with Outward Mode of Electrolyte Flow**

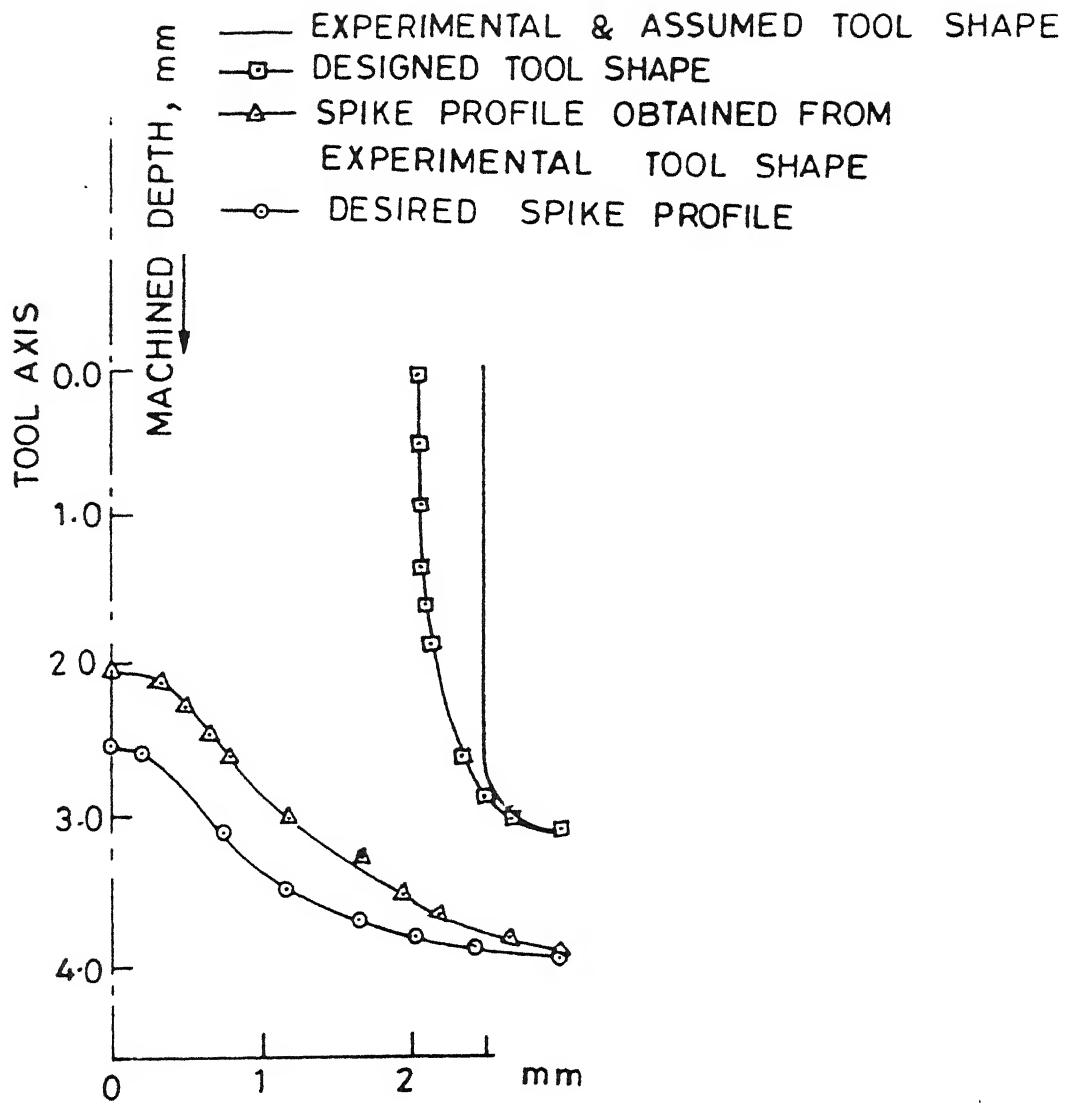Fig. 1·3   A Complete picture of various zones in ECD

Fig. 1.4 Designed Tool for a Desired Spike Profile in Stagnation Zone During ECD

CHAPTER 2

EXPERIMENTATION

2.1 Experimental Setup:

Experiments were conducted on a MICO single station deburring machine shown in Fig 2.1. The feed mechanism of the deburring machine has been modified to make it a drilling machine.

The specifications of the machine are

    Maximum current   =   600 A

    Working voltage   =   12 to 30 Volts

    Electrolyte tank capacity = 1000 liters.

A programmable stepper motor controller has been developed for feeding of the tool. A stepper motor is a four phase motor in which one or more phases may be energized. These have to be done in a particular sequence. This sequence is determined by the direction of rotation, and on whether half step or full step is selected.

A stepper motor controller is basically a device which provides the required sequence of steps at the correct rate. In addition it may also select whether idle, normal or high voltage is to be applied.

The controller can be programmed upto six sequence of operation. The programmable function parameters are

1) number of steps

2) idle time

3) time per step

4) half/full step

5) direction of motion.

To allow the user to enter these values a 16 key keyboard has been incorporated. Also a display is provided which is made up of a voltage selector cum manual mode indicator and a four digit display.

A mechanical device has been used for converting the rotary motion of the stepper motor into the linear feed motion for the tool required during drilling operation. The maximum stroke that can be achieved by this device is only 1 inch. A schematic diagram is shown in Fig. 2.2.

2.2 Experimental Details:

Experiments were planned according to the design of experiments. Brass rod of 18mm diameter was used as the tool material. The length of the tool was 10mm. Internal hole (straight and tapered) was provided on the tool for the flow of the electrolyte. The other end of the tool by which it is connected to the feed mechanism had been properly insulated. A typical tool is shown in Fig. 2.3.

16mm x 16mm square high speed steel (H.S.S) in received condition was used as the workpiece. All the four sides of the workpieces were ground and two pieces have been clamped together as shown in Fig. 2.4, so that there is no gap between the two pieces. The work pieces were clamped such that the parting line of the workpieces coincided with the centre of the tool. This has been achieved by means of attaching a straight thin metal strip at the end of the tool and adjusting the workpieces such that the metal strip coincided with the partition line of the two pieces. Machining was done at the centre of the two pieces so that after the experiments are over they can be separated and the

characteristics of the spike can be easily measured.   Photographs
of the workpieces machined is shown in Fig. 2.5.

Sodium Chloride solution was used as the electrolyte.   The
conductivity of the electrolyte was   kept 0.02 $ohm^{-1}mm^{-1}$.   The
electrolyte was pumped through the tool at a pressure of 4 bar.
The flow rate of the electrolyte was 0.00019 m^2/sec.

2.3 Variables and Responses:

The voltage applied, feed rate, tool hole diameter at outlet
and taper angle of the tool hole were considered as   the
controllable   variables   to   study   their   effect   on   the
characteristics of the spike formed during machining. The   details
regarding the selection of the range of variables is given in   the
next chapter.   Voltage was varied from 13.5 V to   19.5 V in 5
steps. The height as well as the width of the spike were   measured
on the shadow graph with a scale of least count of 1micron as
shown in Fig. 2.6.

To evaluate the spike volume, numerical integration technique
has been used.   The spike has been approximated as shown   in   Fig.
2.8 for computation of its volume. The values of y for   different
values of x were found out with an   increment of 0.5mm in the
abscissa. The solution technique used was three dimensional
version of trapezoidal rule making use of the formulae given
below.

Initially the volume of the Ist cylinder is calculated by

$$\pi \left[\frac{x_{n-2} + x_{n-1}}{2} \right]^2 \left[\frac{y_{n-1} + y_{n-2}}{2} \right]$$

The volume of the second cylinder is calculated by

$$\pi \left[\frac{x_n + x_{n-1}}{2} \right]^2 \left[\frac{y_n + y_{n-1}}{2} \right]$$

Then from the volume of the second cylinder the volume of the first cylinder at the same height as that of the second cylinder is subtracted.

i.e. the volume of the sleeve 2 =

$$\pi \left[\left[\frac{x_n + x_{n-1}}{2} \right]^2 - \left[\frac{x_{n-2} + x_{n-1}}{2} \right]^2 \right] \left[\frac{y_n + y_{n-1}}{2} \right]$$

The volume of the sleeve 2 is then added to the volume of the first cylinder. This process is repeated to get the final volume under the curve.

The active tool surfaces were brought to a uniform finish before machining. The active tool surfaces are shown in Fig. 2.9. Machining was done for a constant depth of 10 mm in each experiment which was controlled by the stepper motor controller.

2.4 Design of Experiments:

The experimental work carried out to study the effects of different variables on the responses is planned in accordance with the statistical technique of experimental design. According to Adler, Markova and Gravosky [7] the design of an experiment is the procedure of selecting the number of trials and conditions for running them, essential and sufficient for solving the problem that has been set with the required precision. The following features are of great importance,

1) Striving to minimize the total number of trials,

2) The simultaneous variation of all the variables determining a process according to special rules called algorithms,

3) The use of a mathematical apparatus formalizing many actions of the experimenter,

4) The selection of a clear cut strategy permitting the experimenter to make substantial decisions after each series of trials or experiments.

The problem for whose solution the design of experiments can be used are exceedingly diverse. With a well designed experiment it is possible to determine accurately, with much less effort, the effect of change in one variable on the process output (also known as the response or yield) and the interaction effect between the different factors if any. If all the investigated factors are quantitative in nature, then it is possible to approximate the response y_n as a polynomial equation.

$$y_n = b_0 + \sum_{i=1}^{k} b_i x_i + \sum_{i=1}^{k} b_{ii} x_i^2 + \sum_{i<j} b_{ij} x_i x_y \qquad (2.1)$$

where x_i (i=1,2,.....k) are coded levels of k quantitative variables and b_0, b_1 etc are the least square estimates of the regression coefficients. The polynomial in the above equation is also known as regression function and the first term under the summation sign pertains to linear effects, the second term under the summation sign pertains to quadratic effects and the third term pertains to interaction effects of the investigated parameters. From the initial experiments it was observed that the linear model is not adequate. Since the F-ratio of second order design lies within the stipulated value a second order polynomial equation is selected here.

2.5 Plan of Experiments:

It was decided to study the influence of four independent parameters viz, the diameter of the hole drilled in the centre of the tool for electrolyte supply, the taper angle of the hole, the applied voltage across the tool and workpiece and feed rate. In order to study the effects a second order polynomial surface equation (2.1) as above is adopted [8].

To estimate the values of the coefficients, in equation (2.1) a central composite rotable design was employed. The plan of the experimentation is described in Table 2.1 and the selection of the factor limits was done as per Table 2.2.

2.6 Response Surface Equations:

A mathematical model for the second order response surface would be of the following form

$$
\begin{aligned}
y = b_0 &+ b_1 x_1 + b_2 x_2 + b_3 x_3 + b_4 x_4 + b_{11} x_1^2 + b_{22} x_2^2 + b_{33} x_3^2 + \\
&b_{44} x_4^2 + b_{12} x_1 x_2 + b_{13} x_1 x_3 + b_{14} x_1 x_4 + b_{23} x_2 x_3 + b_{24} x_2 x_4 \\
&+ b_{34} x_3 x_4
\end{aligned}
\tag{2.2}
$$

where y is the response, $x_1 \ldots \ldots x_4$ are the process parameters and b_0, $b_1 \ldots \ldots b_{34}$ are the coefficients to be calculated.

Thirty one simultaneous equations were obtained from the design matrix (Table 2.1) and these were represented in matrix form as

$$
[y]_{31 \times 1} = [x]_{31 \times 15} [b]_{15 \times 1}
\tag{2.3}
$$

where $[y]$ is the response matrix, $[x]$ is the matrix of variables and $[b]$ is the matrix of coefficients. The least square estimates of the $[b]$ coefficients were determined by

$$[b] = \left[[x^T][x]\right]^{-1} [x]^T [y] \qquad (2.4)$$

Making use of this equation, the coefficients for the model were calculated. A software programme using NAG routines was developed which is given in Appendix 1.

The analysis of variance was carried out for each of the responses separately. In the analysis of variance it is usually of interest to partition the sum of squares of the y's into the contribution due to the first order terms, the additional contribution due to the second order terms, a lack of fit component which measures the deviations of the responses from the fitted surface and finally a measure of the experimental errors obtained from the replicated points at the centre. General formulae for the sum of square are as follows:

	Sum of Squares	Degrees of freedom
Ist Order Terms:	$\sum_{i=1}^{k} b_i (iy)$	k
IInd Order Terms:	$b_o (0y) + \sum_{i=1}^{k} b_{ii} (iiy) + \sum_{i<j} b_{ij} (ijy) - G^2/N$	$k(k+1)/2$
Lack of fit:	found by subtraction	$n_2 - k(k+3)/2$
Experimental error:	$\sum (y_{1u} - \bar{y}_1)^2$	$n_1 - 1$
Total	$\sum_{u=1}^{N} y_u^2 - G^2/N$	$n_1 + n_2 - 1$

In the formulae G is the grand total, N the number of points and y_{1u} represents the responses at the central points with mean $\bar{y}_1$. Accordingly the values of the regression coefficients, their sum of squares and the analysis of variance for the three responses

are given in Tables 2.3, 2.4 & 2.5.

2.7 Testing the Homogenity of Variances

The homogenity of variances is tested with the aid of various statistical data. The simplest of them is the Fisher ratio (F ratio) designed for comparing two variances. The *F ratio is the ratio of mean sum of squares due to lack of fit to the mean sum of squares due to experimental errors.* The value obtained is compared with the tabulated value of the F-ratio.

If the F-ratio obtained for variances is greater than the tabulated value for the corresponding degrees of freedom and the selected significance level, this means *that the variances significantly differ from each other* i.e, *that they are not homogeneous.*

Here also the F-ratio has been calculated for the the models and they are found to be within 95% confidence limits.

For the spike volume model

$$F\text{-ratio} \quad = \quad \frac{312.9775}{76.9402} = 4.06$$

For the spike width model

$$F\text{-ratio} \quad = \quad \frac{0.33166}{0.0823} = 4.02$$

For the spike height model

$$F\text{-ratio} \quad = \quad \frac{0.3804}{0.1041} = 3.65$$

Since all the F ratios are less than $F_{0.05, 10, 6} = 4.08$ the models are found to be adequate within 95% confidence limits.
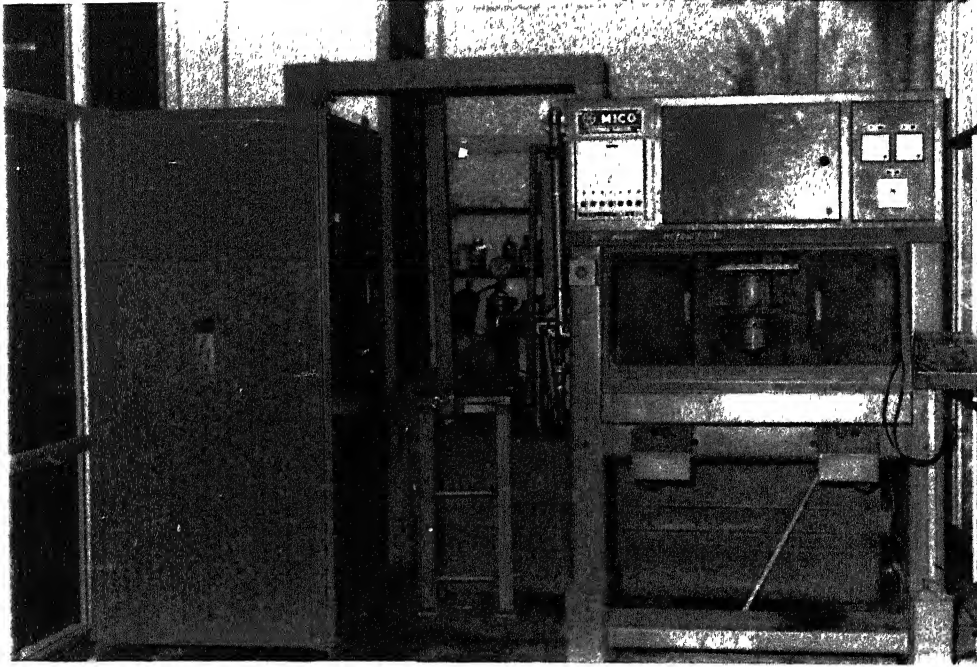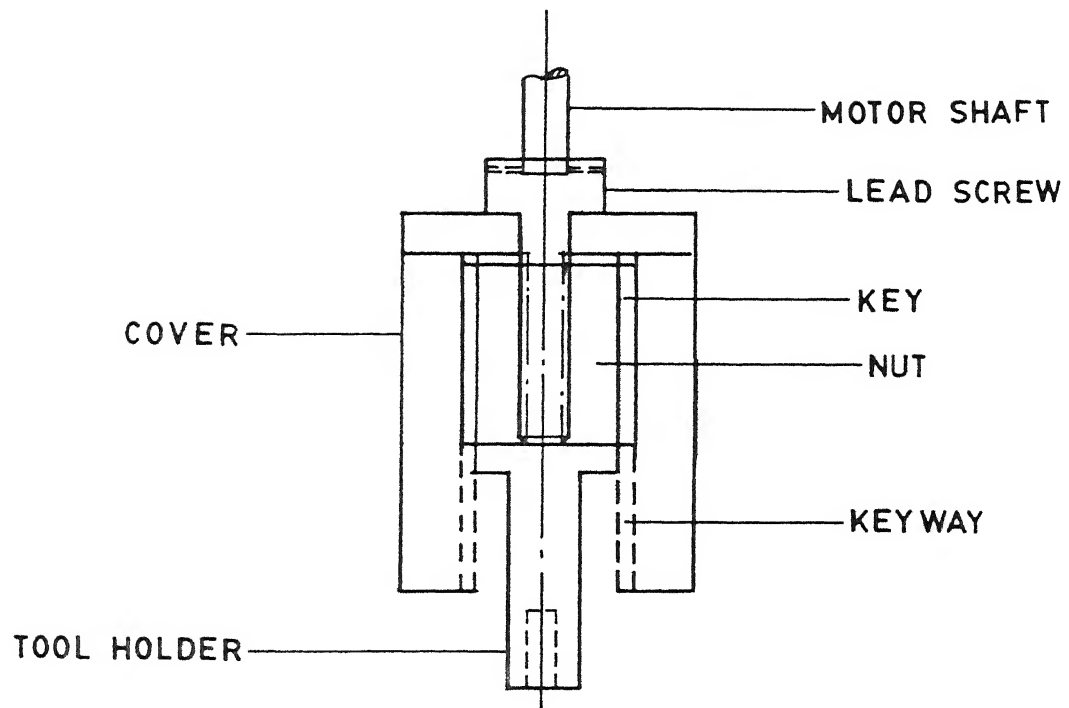
Fig. 2.1   Photograph of Experimental Setup

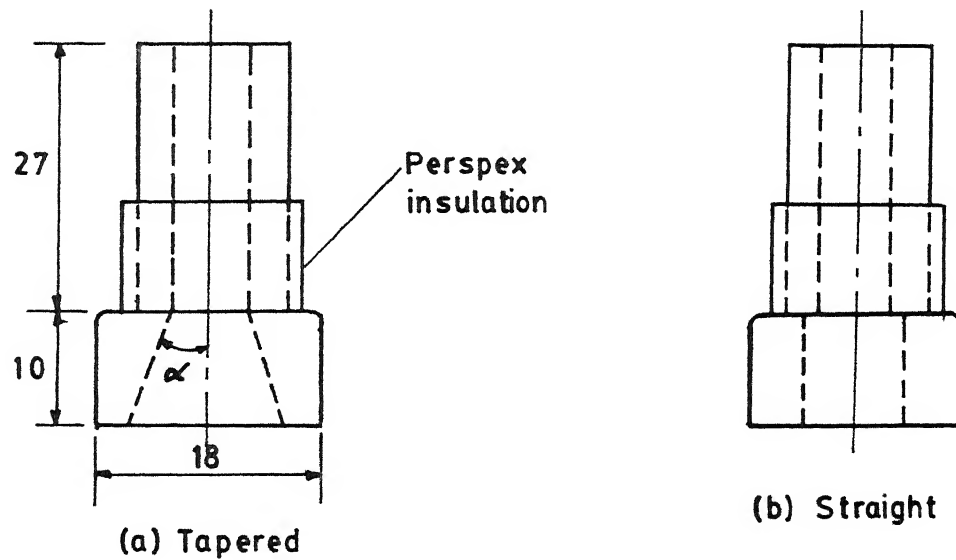Fig. 2·2 Schematic diagram of feed mechanism

MOTOR SHAFT

LEAD SCREW

KEY

NUT

KEYWAY

COVER

TOOL HOLDER

27

10

18

Perspex insulation

α

(a) Tapered

(b) Straight

Fig. 2·3 Schematic diagram of tools

CLAMP — WORK PIECES

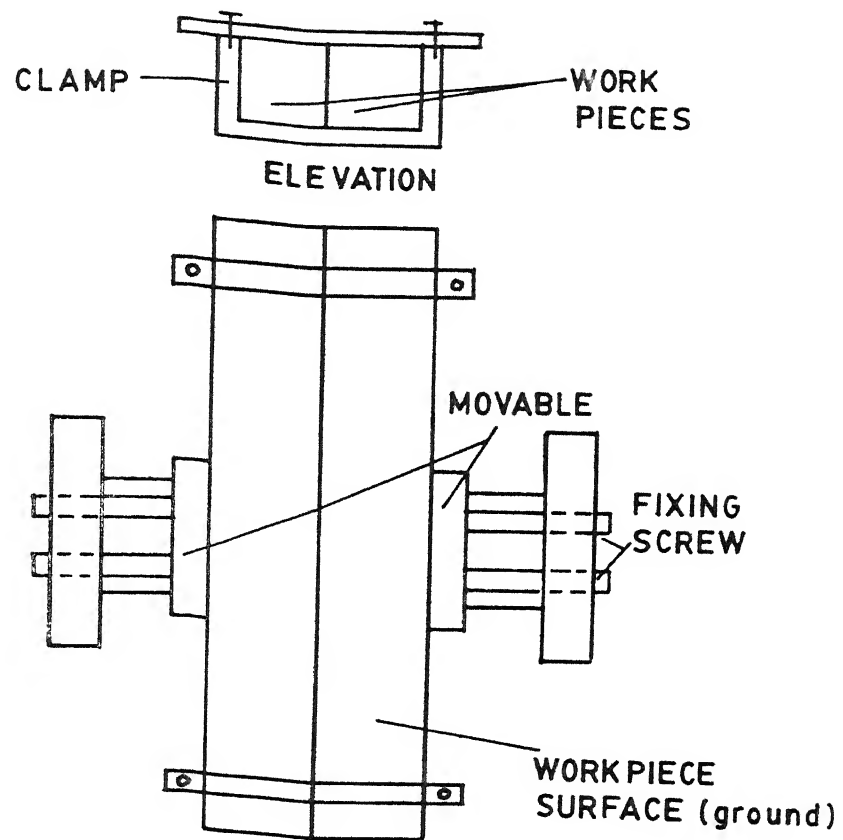ELEVATION

MOVABLE

FIXING SCREW

WORK PIECE SURFACE (ground)
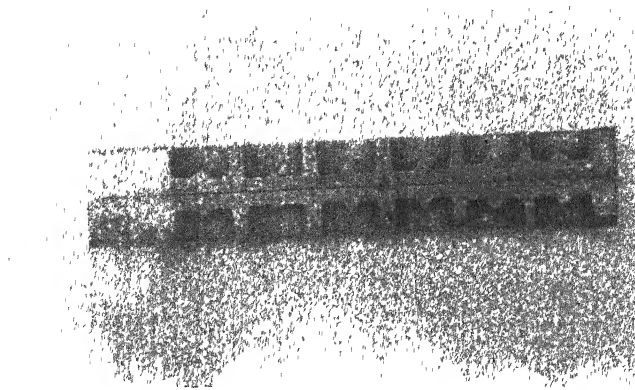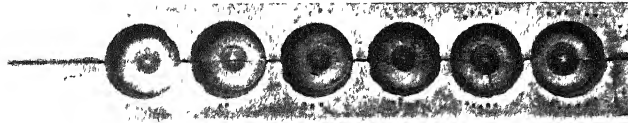
Fig. 2.4 Arrangement for holding the workpiece
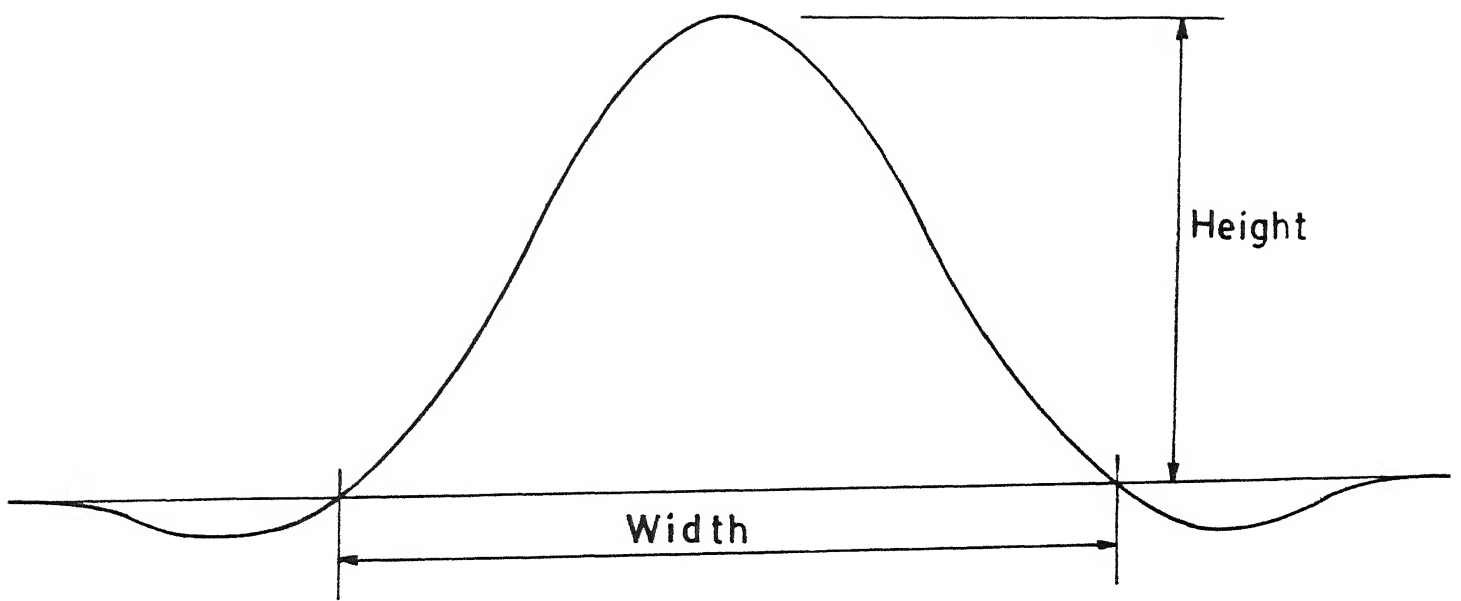
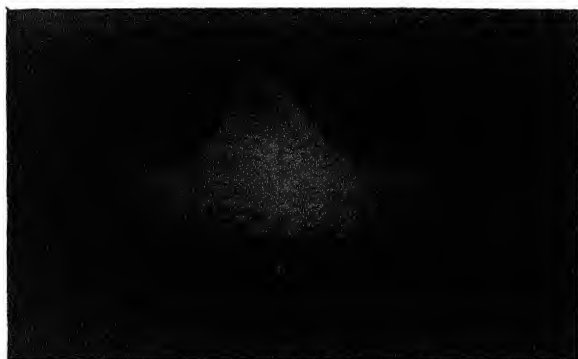Fig. 2.5   Photograph of Machined Workpiece

Fig. 2·6   Spike height and width measurement

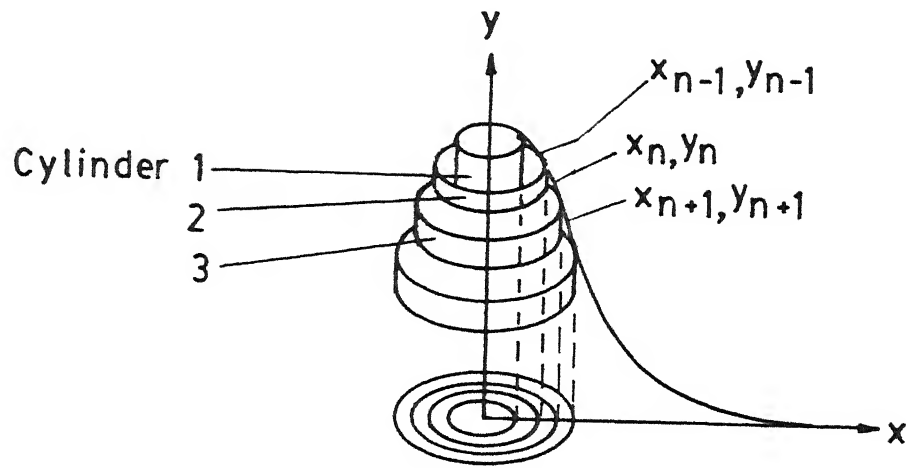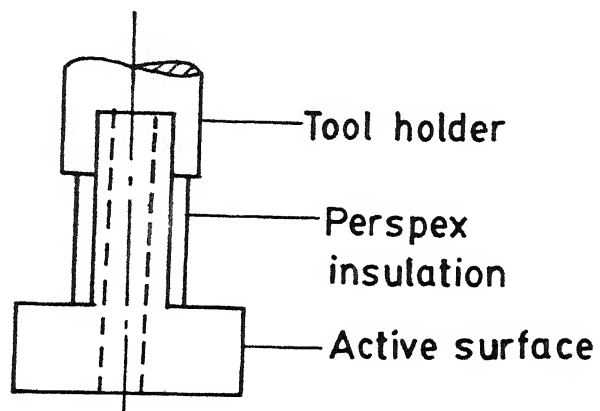2.7 Photograph of Spike

Fig. 2·8 Calculation of spike volume

Fig. 2·9 Active surface of tool

Table 2.1

Plan of Experimentation

Central Composite rotable second order designs

4 x variables   N = 31 treatment combinations

No.	x_1	x_2	x_3	x_4	Responses		
					Width mm	Height mm	Volume mm^3
1	−1	−1	−1	−1	5.5915	2.6345	20.319
2	1	−1	−1	−1	7.9205	4.603	110.0067
3	−1	1	−1	−1	5.23	1.8305	21.207
4	1	1	−1	−1	6.9595	3.89	42.629
5	−1	−1	1	−1	4.412	1.179	10.277
6	1	−1	1	−1	8.2965	3.853	85.687
7	−1	1	1	−1	5.1995	1.3745	16.4525
8	1	1	1	−1	6.48	2.7823	39.8332
9	−1	−1	−1	1	5.7055	4.16	39.79
10	1	−1	−1	1	8.424	6.7345	171.9948
11	−1	1	−1	1	5.8	3.693	33.74
12	1	1	−1	1	8.2765	6.9955	117.908
13	−1	−1	1	1	5.5335	3.529	32.045
14	1	−1	1	1	7.972	6.078	160.0027
15	−1	1	1	1	5.403	2.941	31.9102
16	1	1	1	1	8.163	6.668	149.728
17	−2	0	0	0	4.537	1.67	12.759
18	2	0	0	0	8.732	5.238	132.42
19	0	−2	0	0	6.1765	3.5945	52.984
20	0	2	0	0	7.089	3.3875	66.1889
21	0	0	−2	0	5.8375	3.4725	34.123
22	0	0	2	0	6.836	3.7755	49.167
23	0	0	0	−2	6.625	1.1455	17.8315
24	0	0	0	2	7.0785	6.368	123.1936
25	0	0	0	0	7.0925	4.126	77.662
26	0	0	0	0	6.451	4.313	56.5938
27	0	0	0	0	6.4585	3.8785	56.1416
28	0	0	0	0	6.6015	4.751	69.01
29	0	0	0	0	6.674	4.626	64.186
30	0	0	0	0	6.682	4.175	55.779
31	0	0	0	0	6.23	3.984	55.057

Table 2.2

Selection of Factor Levels

Factor Name	Abbreviations	Levels				
		+2	+1	0	-1	-2
Tool hole diameter for electrolyte flow, mm	(x_1)	10	9	8	7	6
Taper angle of the tool hole, degrees	(x_2)	12	9	6	3	0
Applied Voltage, Volts	(x_3)	19.5	18	16.5	15	13.5
Feed rate, mm/min	(x_4)	1.2	1.03	0.85	0.67	0.5

Table 2.3

Regression Coefficients, Sum of Squares and Analysis of

Variance - Spike Volume

Values of Regression Coefficients		Sum of Squares	
b_0	62.06	(0y)	2066.6
b_1	37.97	(1y)	911.37
b_2	-6.26	(2y)	-150.31
b_3	-0.065	(3y)	- 1.575
b_4	25.06	(4y)	601.43
b_{11}	3.74	(11y)	1664.3
b_{22}	0.487	(22y)	1560.2
b_{33}	-3.99	(33y)	1416.7
b_{44}	3.22	(44y)	1647.6
b_{12}	-11.15	(12y)	-178.47
b_{13}	1.07	(13y)	17.086
b_{14}	15.76	(14y)	252.25
b_{23}	4.78	(23y)	76.538
b_{24}	2.22	(24y)	35.622
b_{34}	3.26	(34y)	52.164

ANOVA

	S.S	D.F	M.S
First order terms	50255.96098	4	12563.99025
Second order terms	7870.775	10	787.0775
Lack of fit	3269.77507	10	312.9775
Error	449.6413	6	76.9402
Total	61846.1524	30	

Table 2.4

Regression Coefficients, Sum of Squares and Analysis of

Variance - Spike Width

Values of Regression Coefficients		Sum of Squares	
b_0	6.598	(0y)	204.468
b_1	1.167	(1y)	28.007
b_2	-0.021	(2y)	-0.519
b_3	-0.018	(3y)	-0.451
b_4	0.254	(4y)	6.095
b_{11}	0.004	(11y)	158.443
b_{22}	0.0038	(22y)	158.429
b_{33}	-0.07	(33y)	156.061
b_{44}	0.058	(44y)	160.181
b_{12}	-0.195	(12y)	-3.124
b_{13}	0.069	(13y)	1.11
b_{14}	0.073	(14y)	1.17
b_{23}	0.0:5	(23y)	0.407
b_{24}	0.147	(24y)	2.359
b_{34}	0.011	(34y)	0.179

ANOVA

	S.S	D.F	M.S
First order terms	34.2503	4	8.5625
Second order terms	1.4002	10	0.14002
Lack of fit	3.3166	10	0.33166
Error	0.4339	6	0.0823
Total	39.401	30	

Table 2.5

Regression Coefficients, Sum of Squares and Analysis of

Variance - Spike Height

Values of Regression Coefficients

b_0	4.26		(0y)	121.4508
b_1	1.14		(1y)	27.3988
b_2	-0.125		(2y)	-3.0102
b_3	-0.23		(3y)	-5.5302
b_4	1.21		(4y)	29.0972
b_{11}	-0.144		(11y)	90.5778
b_{22}	-0.134		(22y)	90.8738
b_{33}	-0.101		(33y)	91.9378
b_{44}	-0.068		(44y)	92.9998
b_{12}	0.045		(12y)	0.7308
b_{13}	0.028		(13y)	0.4528
b_{14}	0.253		(14y)	4.0432
b_{23}	0.053		(23y)	0.8498
b_{24}	0.136		(24y)	2.1882
b_{34}	0.087		(34y)	1.4022

ANOVA

	S.S	D.F	M.S
First order terms	68.2071	4	17.0518
Second order terms	2.7285	10	0.2728
Lack of fit	3.8036	10	0.3804
Error	0.6246	6	0.1041
Total	75.3638	30	

CHAPTER 3

RESULTS AND DISCUSSION

The experimental results obtained and their interpretations have been discussed in this chapter.

Careful running of an experiment is undoubtedly the main condition for the success of an investigation. This is a general rule, and the design of an experiment is not an exception to it.

Quite a few preliminary experiments were conducted to study the feasibility of the conceived concept, to distinguish the potential variables that would affirm prominent influence on the responses and to fix the working range of the selected variables. Under stable conditions of machining the obtained responses were observed to be repeatable within reasonable limits.

The ultimate objective of any machining is to produce a component with certain characteristics like dimensional as well as form accuracy in reasonable machining time. So this study is directed to find the characteristics of spike formed during electrochemical drilling and to minimize its volume within the experimental range.

3.1 Selection of Parameters and their Range:

The width of the spike formed will have a direct relationship to the outlet tool hole diameter of the electrolyte flow path. Generally current density of the order of 50 A/cm^2 is employed for electrochemical drilling. The maximum current that can be drawn from the machine being 200 A, in order to keep the current density within the abovesaid value the tool hole outlet diameter was kept in the range of 6 to 10 mm. Here the current density for the

tools varies in the range of 50-72 A/cm^2. If the electrolyte path is tapered then the machining of spike will take place more effectively which will reduce the height of the spike. But if the taper angle is increased arbitrarily, discontinuities in the electrolyte flow will take place. The electrical energy input required for the process has been varied by changing the applied voltage.

The available voltages in the machine ranges from 12 to 24 V only. In addition the feed rate of the tool was observed to influence the above machined responses. A feed rate of zero will usually denote deburring operation. Maximum feed rate in any ECM operation is fixed by short circuiting and/or electrolyte boiling. With the above in view the experimental range of feed rate employed in the present investigation has been from 0.5 to 1.2 mm/min.

3.2 Response Surface Coefficients:

Making use of the equation for the response (equation 2.2) the regression coefficients were calculated for spike volume. width and height. For this purpose a computer program has been developed using NAG subroutines from the NAG library and is shown in Appendix 1. The values of the regression coefficients are shown in Tables 2.3, 2.4 and 2.5 together with their sum of squares.

The analysis of variance (ANOVA) was carried out for each of the models. The adequacy of the models were tested by evaluating the F coefficients. Since all the three F-ratios are less than the tabulated value of $F_{0.05,10,6}$ =4.08, the models are found to be adequate within 95% confidence limits which is used in

technical problems.

3.3 Process Optimization:

An attempt has been made to find the optimum value of variables which will minimize the spike volume subject to the ranges of design variables within the experimental region. Since the width and height of the spike follows from its volume, only the spike volume has been minimized.

After the quadratic surface has been fitted, the position of the minimum value of $\hat{y}$ (here the spike volume) is found by differentiating with respect to each variable in turn [8]. With four factors the surface is represented by

$$\hat{y} = b_0 + b_1 x_1 + b_2 x_2 + b_3 x_3 + b_4 x_4 + b_{11} x_1^2 + b_{22} x_2^2 + b_{33} x_3^2 +$$
$$b_{44} x_4^2 + b_{12} x_1 x_2 + b_{13} x_1 x_3 + b_{14} x_1 x_4 + b_{23} x_2 x_3 + b_{24} x_2 x_4$$
$$+ b_{34} x_3 x_4 \tag{3.1}$$

$$\frac{\partial \hat{y}}{\partial x_1} = b_1 + 2b_{11} x_1 + b_{12} x_2 + b_{13} x_3 + b_{14} x_4 = 0 \tag{3.2}$$

$$\frac{\partial \hat{y}}{\partial x_2} = b_2 + b_{12} x_1 + 2b_{22} x_2 + b_{23} x_3 + b_{24} x_4 = 0 \tag{3.3}$$

$$\frac{\partial \hat{y}}{\partial x_3} = b_3 + b_{13} x_1 + b_{23} x_2 + 2b_{33} x_3 + b_{34} x_4 = 0 \tag{3.4}$$

$$\frac{\partial \hat{y}}{\partial x_4} = b_4 + b_{14} x_1 + b_{24} x_2 + b_{34} x_3 + 2b_{44} x_4 = 0 \tag{3.5}$$

The solutions of these 4 simultaneous equations are denoted by x_{1s}, x_{2s}, x_{3s} and x_{4s} respectively. The solutions in coded values and corresponding actual values are given in Table 3.1.

For further study of the response surface, some transformations of the x-variables simplify the task. The origin of the x-co-ordinates can be transferred to the stationary point

by making the transformations

$$x_1' = x_1 - x_{1o}; \quad x_2' = x_2 - x_{2o}; \quad x_3' = x_3 - x_{3o}; \quad x_4' = x_4 - x_{4o}$$

With this substitution the linear terms disappear from the quadratic expression, which becomes

$$\hat{y} = \hat{y}_s + b_{11} x_1'^2 + b_{22} x_2'^2 + b_{33} x_3'^2 + b_{44} x_4'^2 + b_{12} x_1' x_2' + b_{13} x_1' x_3'$$
$$+ b_{14} x_1' x_4' + b_{23} x_2' x_3' + b_{24} x_2' x_4' + b_{34} x_3' x_4' \qquad (3.6)$$

where, $\hat{y}_s = b_0 + \dfrac{1}{2} \left[b_1 x_{1o} + b_2 x_{2o} + b_3 x_{3o} + b_4 x_{4o} \right]$ $\qquad$ (3.7)

is the estimated minimum value of $\hat{y}$.

On substitution of the values on the above equation the minimum value of y (spike volume) is found to be 12.4225 mm^3.

3.4 Effect of Feed Rate on Spike Characteristics:

Variation of spike volume, spike height and spike width with respect to feed rate at constant voltage and tool hole taper angle for different tool hole diameters are shown in Fig. 3.1, 3.2 and 3.3 respectively.

The variation of spike volume with respect to feed rate is more or less constant for a tool diameter of 6mm. For the other tool diameters tested there is some marked increase in spike volume with increase in feed rate. The slope of the spike volume vs feed rate characteristics is found to increase with increasing tool hole diameter. Electrochemical deburring which employs a static electrode and corresponds to zero feed rate condition would give insignificant spike for any tool hole diameter. This physical concept is evident from the extrapolation of the characteristics. It is rather obvious that the spike volume would

increase for increasing tool hole diameter. It is apparent that there is an optimum feed rate for maximum material removal rate with a constraint on the permissible spike volume.

The spike height and spike width increase both with increase in feed rate as well as tool hole diameter. Nevertheless the feed rate has a less pronounced effect on spike width than on spike height. Decreasing the feed rate to approach zero feed rate condition would reduce the spike height drastically but will have minimal influence on the spike width.

Variation of spike volume, spike height and spike width with respect to feed rate at constant voltage and tool hole diameter for different tool hole taper angles are given in Fig. 3.4, 3.5 and 3.6 respectively.

The spike volume and feed rate characteristics at various tool hole taper angles reveals the fact that the spike volume decreases with increase in tool hole taper angle. This is evident from the Fig. 3.7. In Fig. 3.7(a) for which the taper angle θ = 0, in spite of the tool being given a feed rate f, the spike volume would experience zero feed rate conditions, with if at all any machining taking place due to stray current effects. In the second case the tool would exert its influence and machine the spike where the effective feed rate is a function of f and θ. This decreases the spike volume. With increasing feed rate, the different taper angle characteristics appear to converge at a particular feed rate although it is outside the experimental conditions considered. For minimum spike volume it is expedient to employ maximum taper angle provided it does not create serious disturbances for effective flow of electrolyte.

The variation of spike height with feed rate at different tool hole taper angles shows a monotonous increase in spike height with increase in feed rate. But the variation of spike width at different tool hole taper angles intersect at a feed rate of 0.88 mm/min (approximately). Below this particular feed rate for minimum spike width the taper angle should be increased and above this feed rate the tool inside taper angle should be decreased to achieve the above said effect.

Variation of spike volume, spike height and spike width with respect to feed rate at constant tool hole diameter and tool hole taper angle for different voltages are given in Fig. 3.8, 3.9 and 3.10 respectively. Material removal rate is well known to be dependent on the applied voltage for a constant feed rate, other parameters remaining constant. This trend is exhibited by the feed rate, spike height characteristics at different voltages shown in Fig. 3.9. Spike volume and spike width continuously change with increasing feed rate at different voltages as shown in Fig. 3.8 and 3.10.

3.5 Effect of Tool Hole Diameter on Spike Characteristics:

Variation of spike volume, spike height and spike width with respect to tool hole diameter at different feed rates for a constant tool hole taper angle and applied voltage is shown in Figs. 3.11a,b,c. The spike volume and spike height characteristics exhibit a non-linear trend whereas the spike width is linear and monotonously increasing with tool hole diameter for all feed rates tested.. The spike characteristics are higher for higher feed rates. The effect of feed rate is well pronounced for spike volume and spike height. The feed rate does not influence

spike width to the extend as in the above and this is reasoned intuitively. Tool hole diameter dictates the electrolyte flow velocity in the machining zone for a constant delivery pump. Though the least tool hole diameter could result in the minimum spike volume which is of our interest, the hole diameter employed in actual practice should be a compromise which would ensure effective flow of electrolyte.

3.6 Effect of Tool Hole Taper Angle on Spike Characteristics:

Variation of spike volume, spike height and spike width with respect to tool hole taper angle at different voltages for a constant tool hole diameter and feed rate is shown in Figs. 3.12 a,b,c. The spike volume characteristics show no definite trend. The spike height characteristics indicate the existence of a particular taper angle for which spike height is maximum. However the optimum values are different for different voltages. As the spike width characteristics are for a constant tool hole diameter of 8 mm, the tool hole taper angle hardly exerts any influence on the spike width.

3.7 Effect of Applied Voltages on Spike Characteristics:

Variation of spike volume, spike height and spike width with respect to voltage applied at different tool hole taper angles for a constant tool hole diameter and feed rate are shown in Figs. 3.13 a,b,c. The spike volume characteristics are very much dependent on tool hole taper angle for the voltage range selected. The 0° taper angle curve shows decreasing trend while the 12° taper angle curve increases and then droops down. The curves for the other taper angles employed gets accommodated between these two. The spike height characteristics show a decreasing trend for

all taper angles while the spike width changes not more than a millimeter for the entire voltage range of 13.5 to 19.5 V and taper angle of 0 to 12°.

3.8 Surface Characteristics from Scanning Electron Microscope (SEM) Studies:

The microfinish of an ECM surface is governed mainly by the type of the electrolyte, the composition of workpiece material and the machining conditions such as current density and electrolyte flow rate.

The main factors that lead to a poor surface finish in ECM are pitting and formation of oxide layers. Here the surfaces viz. the spike, the side surfaces of the hole and the base of the hole were studied under SEM at different magnifications after thoroughly cleaning the specimen by ultrasonic means. From the photographs given in Fig. 3.14 the following points can be noted.

1. Pitting of surface has taken place (Fig. 3.14a,b,c)

2. Deposition of granular particles of sodium chloride (Fig. 3.14h)

NaCl solution has got a passivating effect. Pitting normally occurs in regions of low current density where the passivating layer would slow down dissolution of the majority of the surface. Bannard [9] has investigated the surface finish of hole drilling in ECM. He has found that electrochemical drilling of multiphase alloys could present particular problems, where, if the correct dissolution controlling anodic film is not generated, differential dissolution of the phases would occur resulting in a rough surface which has been the case here. However Cole and Hopenfield [10] claims that if the current density is sufficiently large (100 A/cm^2) bright surface finishes could be obtained in metals and

alloys. But here the current density has been in between 50 and 70 A/cm^2. Another reason for pitting is gas evolution at the anode-electrode, the gas bubbles rupture the anodic layer causing localized pitting.

Fig 3.15 shows the photograph and plot from the shadow graph of the drilled hole. It can be seen that at the root of the spike there is a depression formed compared with the flat face of the hole. This can be explained as follows. In the machining zone where the flow velocity is low, increased electrolyte heating will be found, often leading to boiling and thus vapour generation. Boiling and steam generation can also occur where high flow velocities cause low pressures which lower the saturation temperature to the local electrolyte temperature causing cavitation. As the vapour generation rate near the electrode surface is increased a point will be reached where a vapour blanket completely covers a part of the electrode surface. If this blanketed section occurs on the work surface, the surface will be machined to accommodate to the flow pattern and blanketing will stop [11].
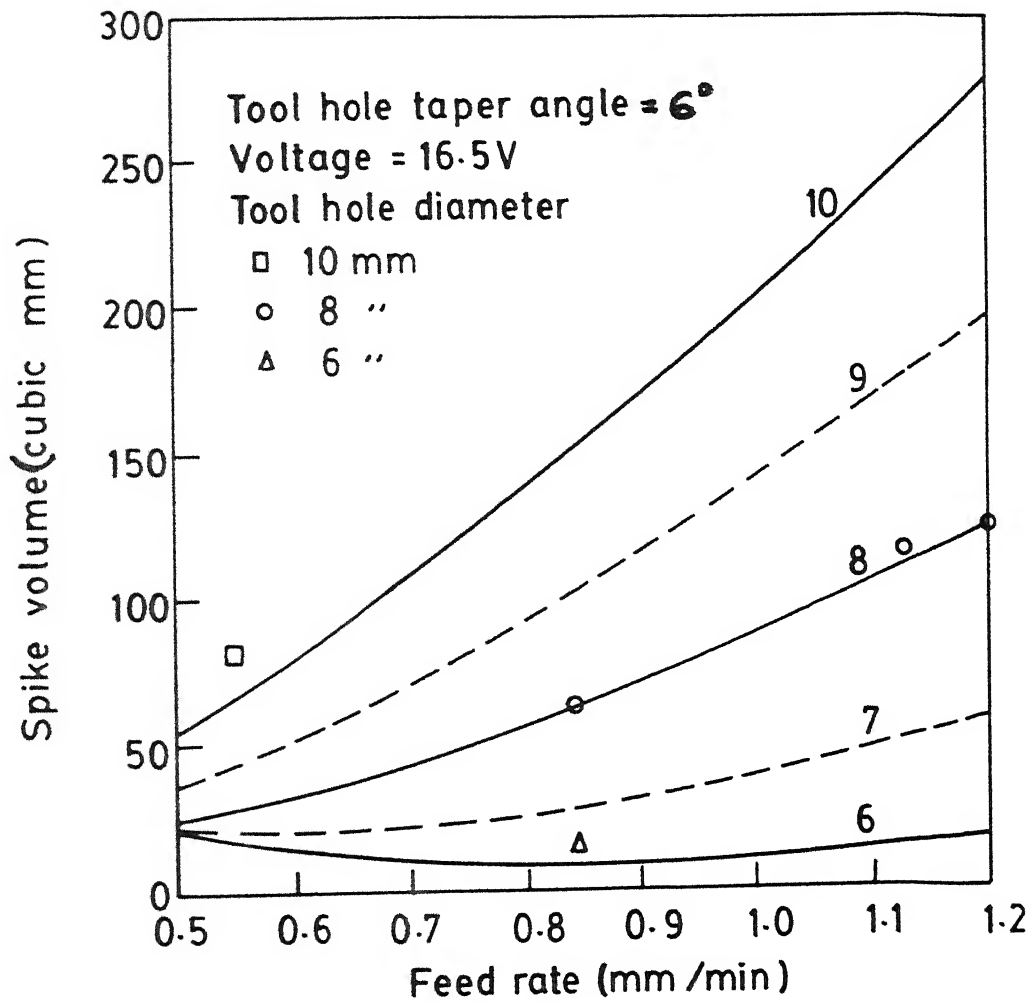
Fig. 3·1 Variation of spike volume with feed rate
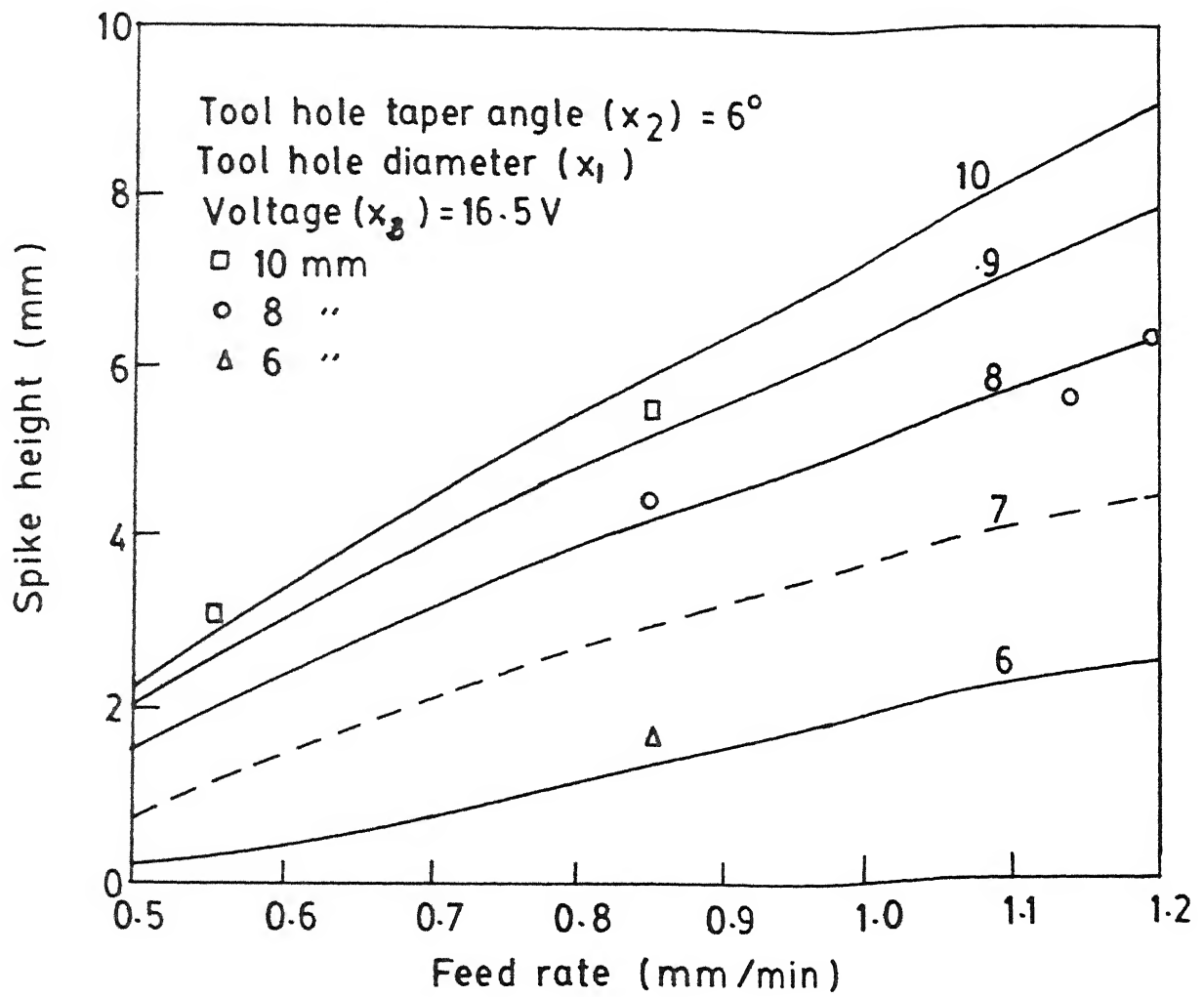
Fig. 3·2 Variation of spike height with feed rate

Fig. 3.4 Variation of spike volume with feed rate
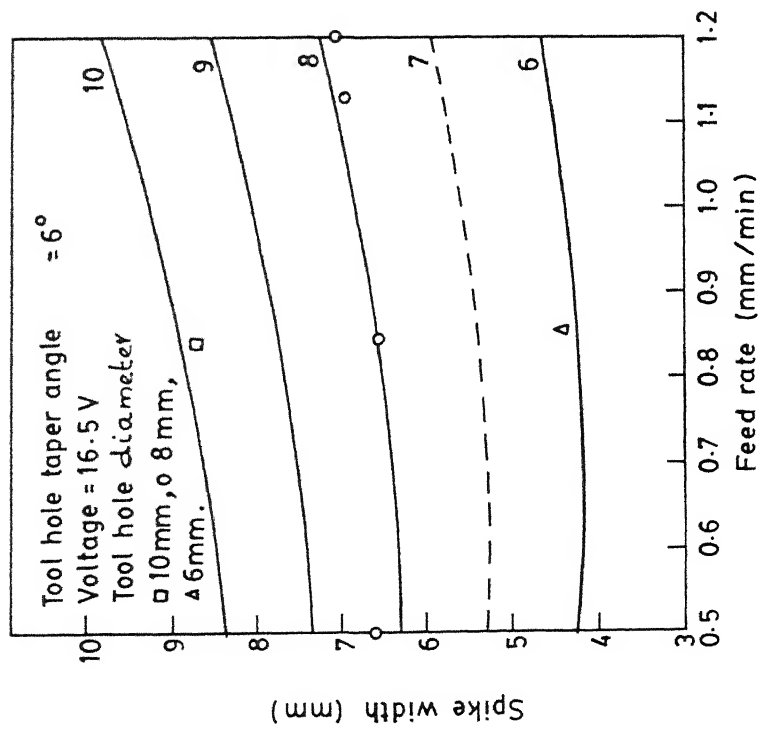
Fig. 3.3 Variation of spike width with feed rate
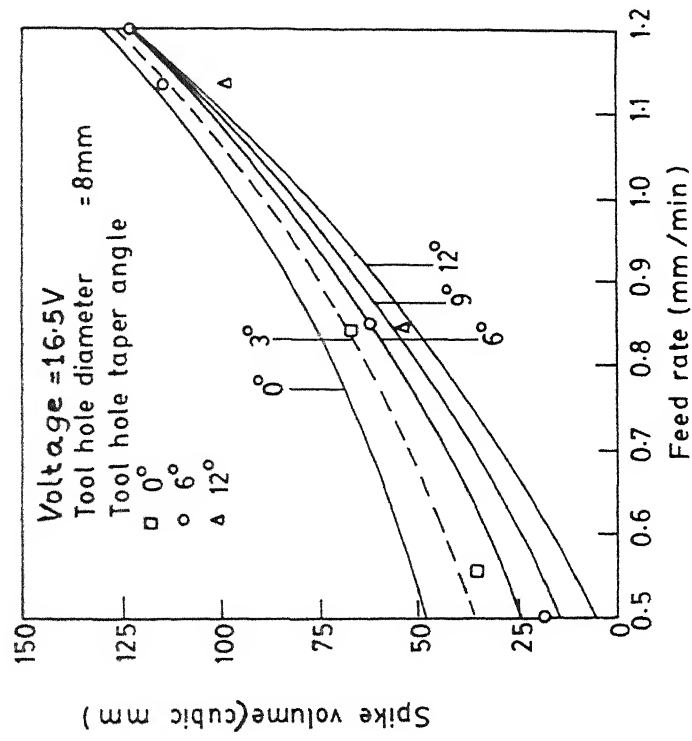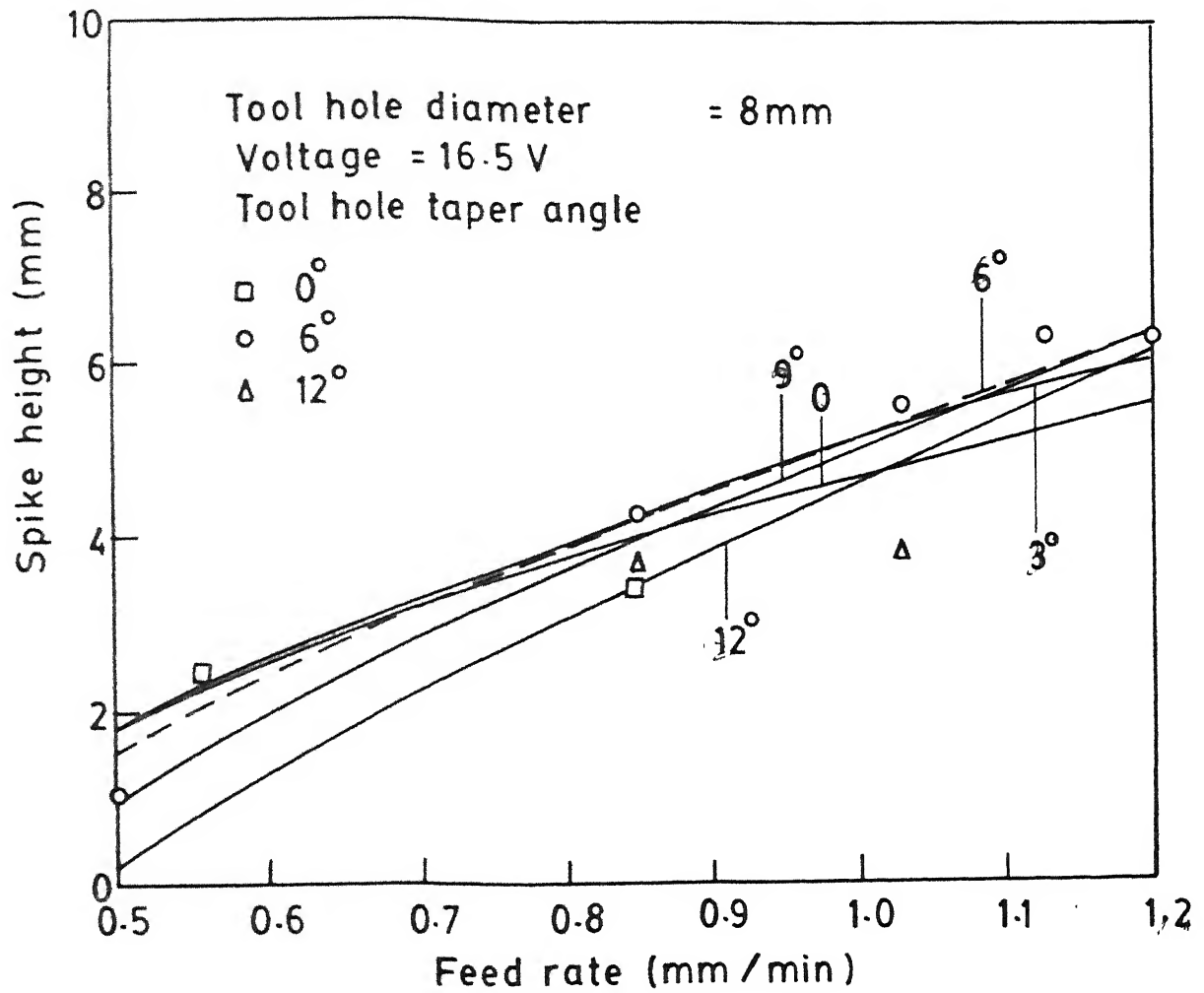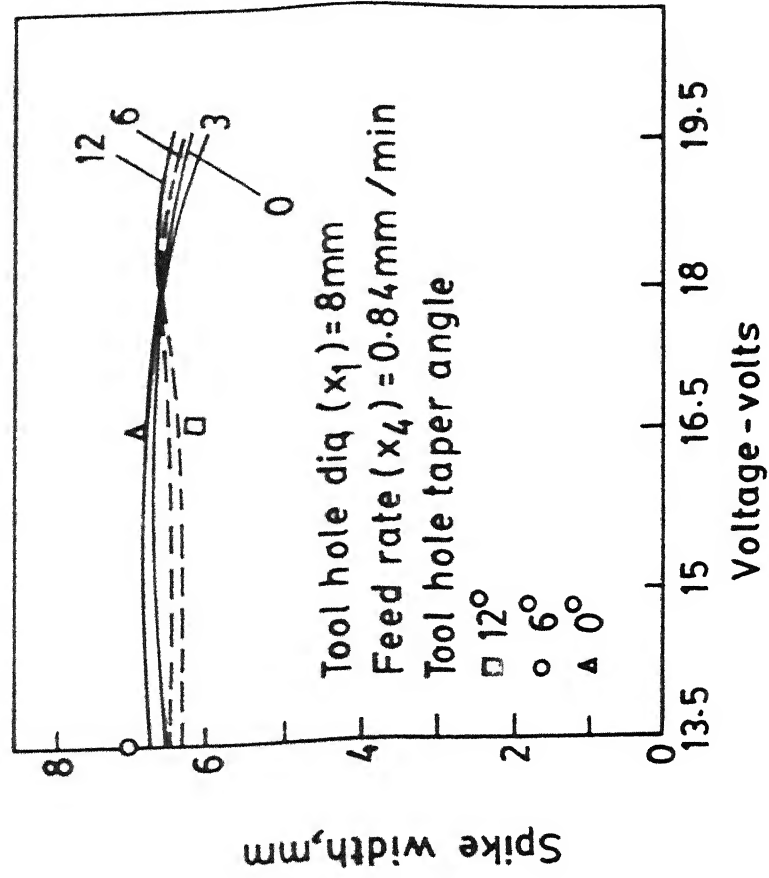
Fig. 3·5   Variation of spike height with feed rate
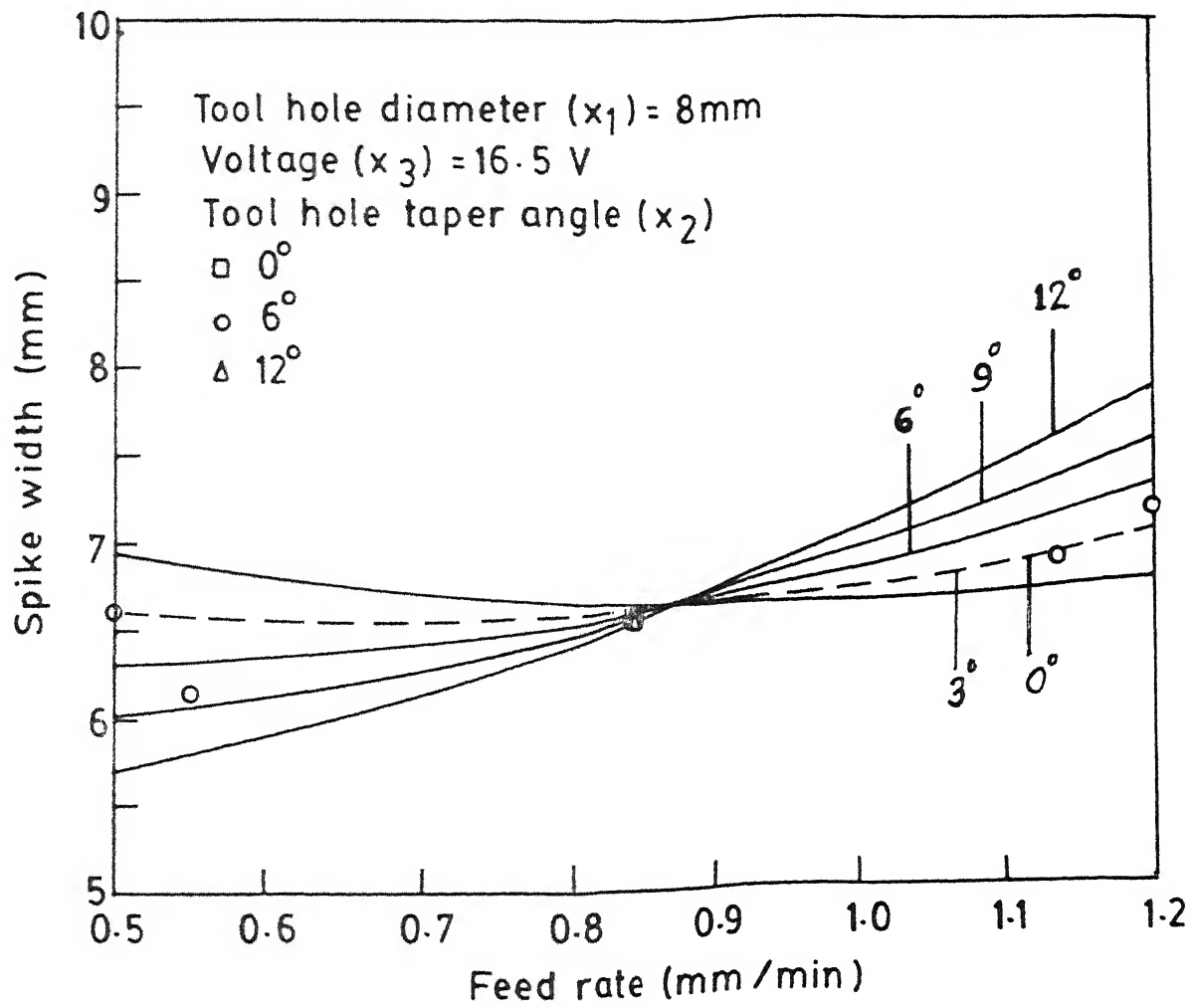
Fig. 3·6 Variation of spike width with feed rate

(a) Straight holed tool   (b) Tapered holed tool
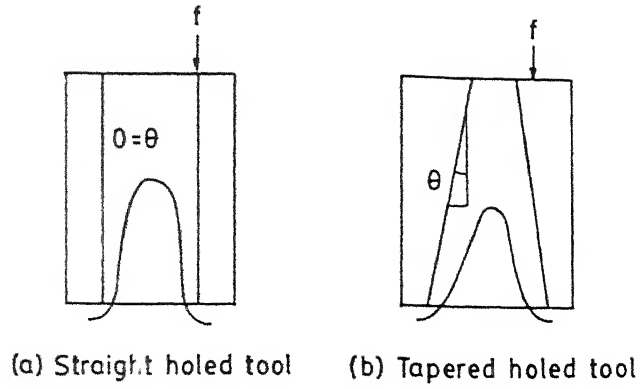
Fig. 3·7 Spike characteristics
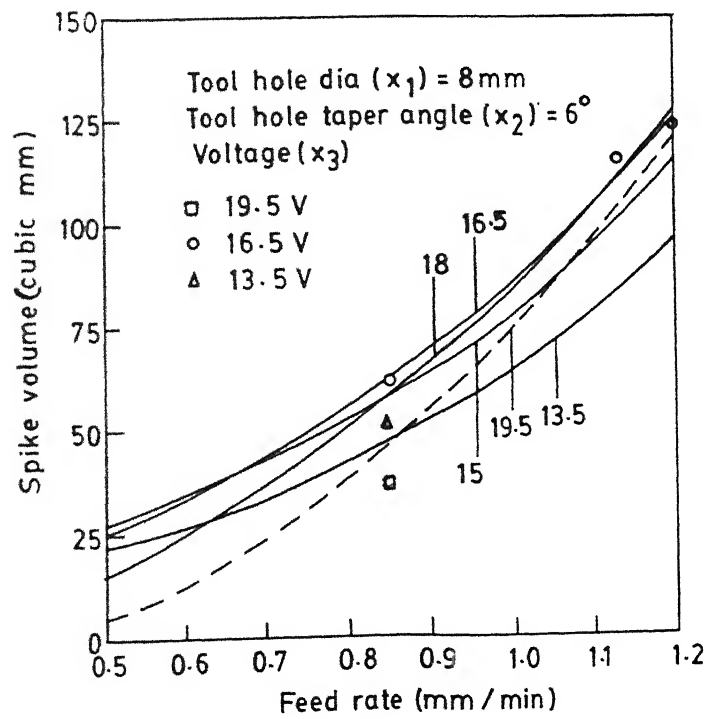
Fig. 3·8 Variation of spike volume with feed rate
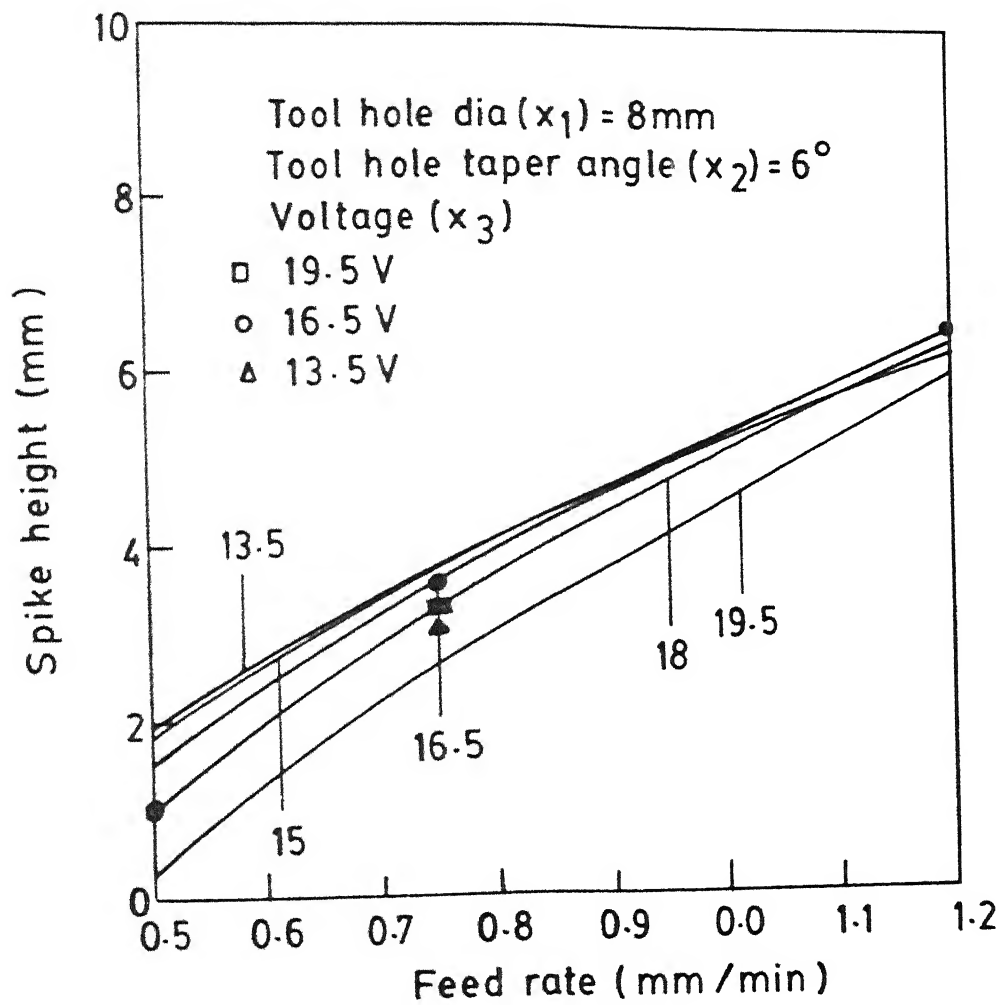
Fig. 3·9 Variation of spike height with feed rate
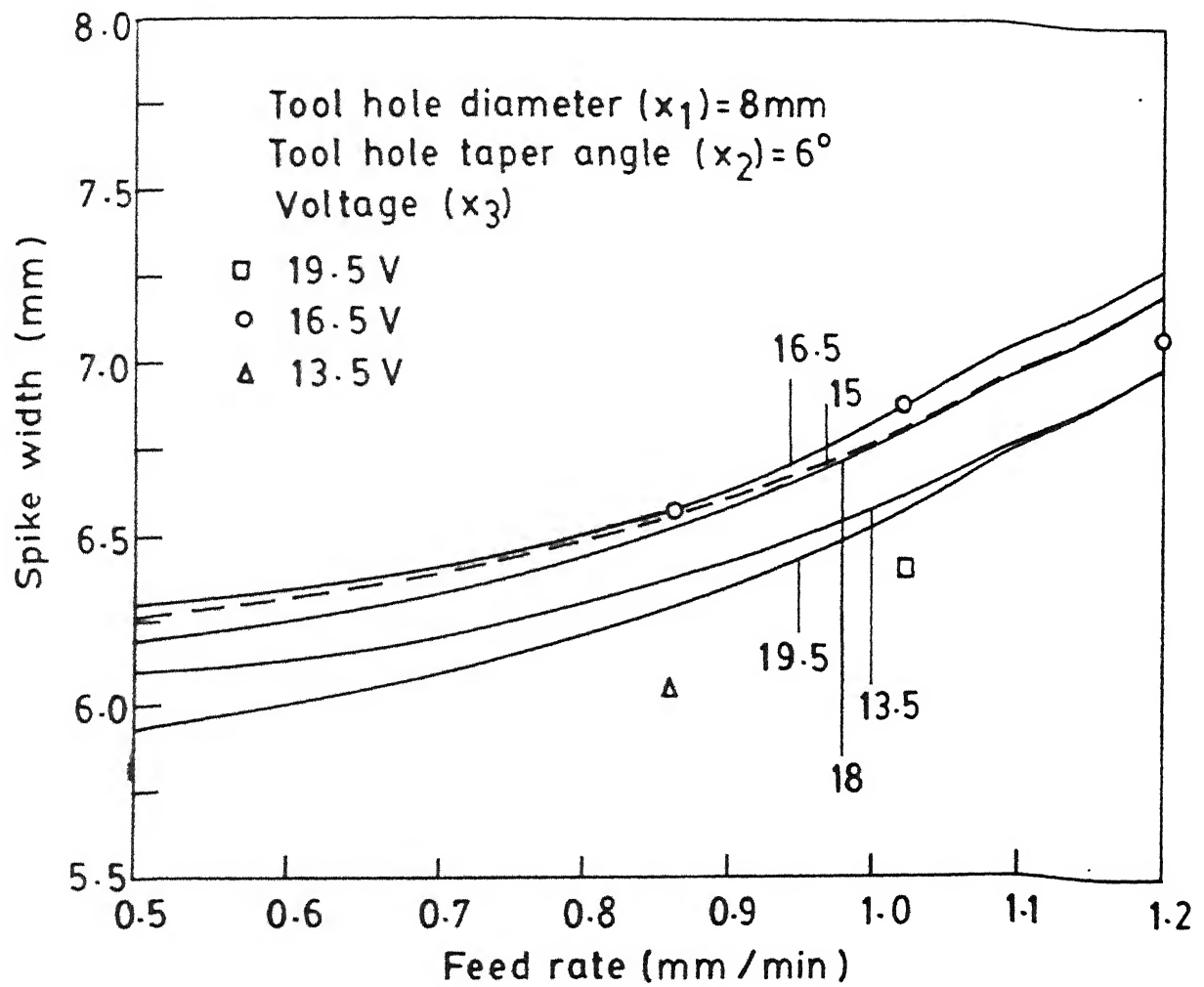
Fig. 3·10 Variation of spike width with feed rate
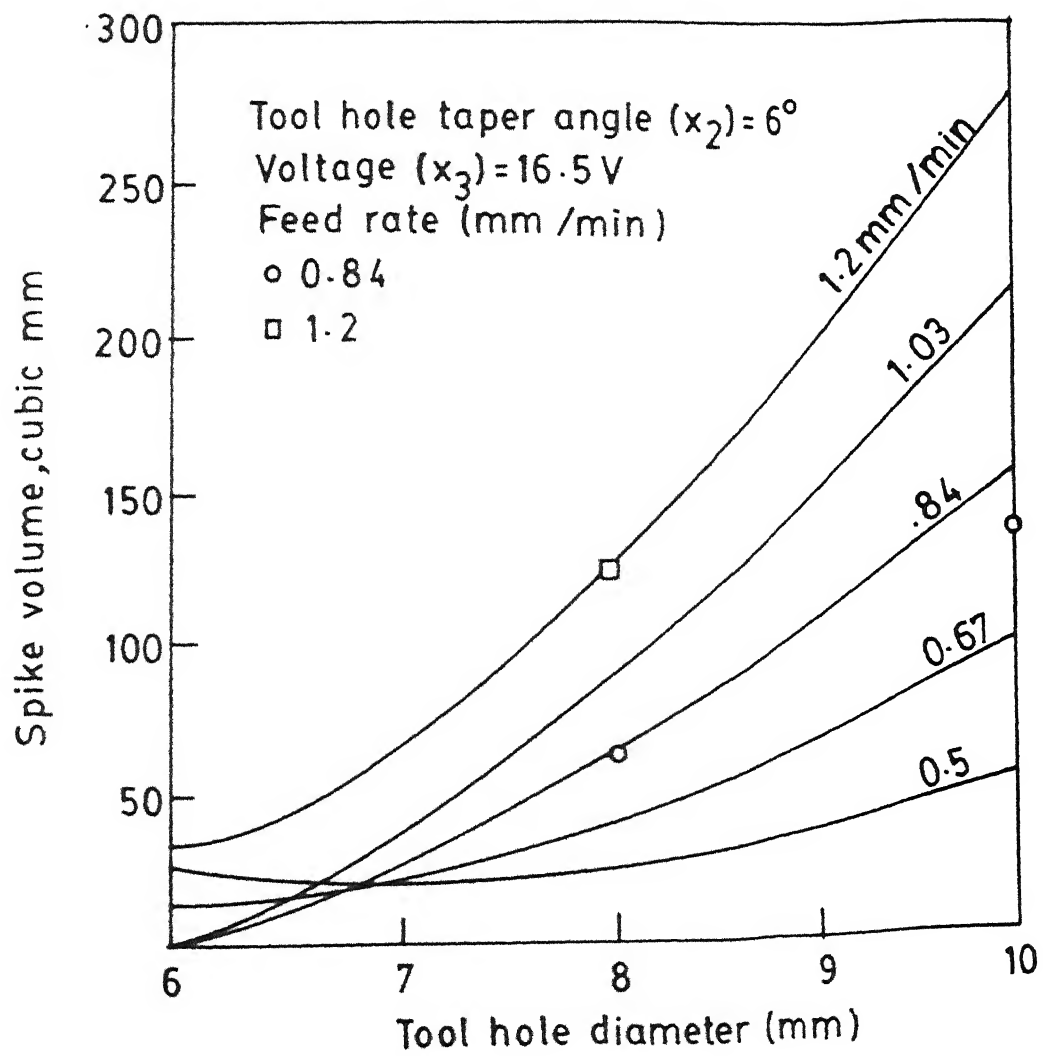
Fig. 3·11a   Variation of spike volume with tool hole diameter

Fig.3.11c Variation of spike width with tool hole dia
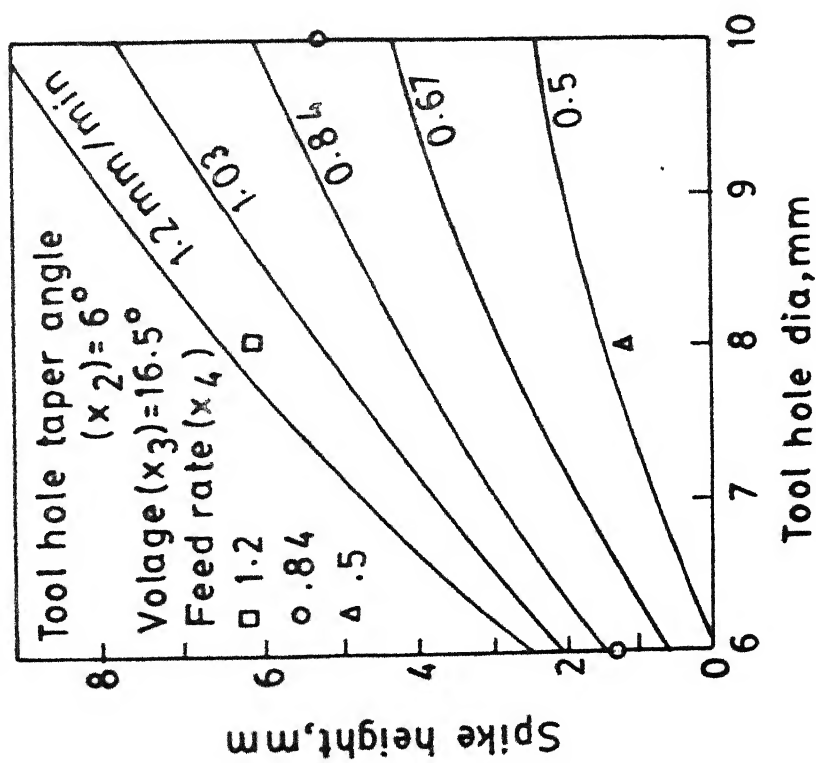
Fig. 3.11(b) Variation of spike height with tool hole dia
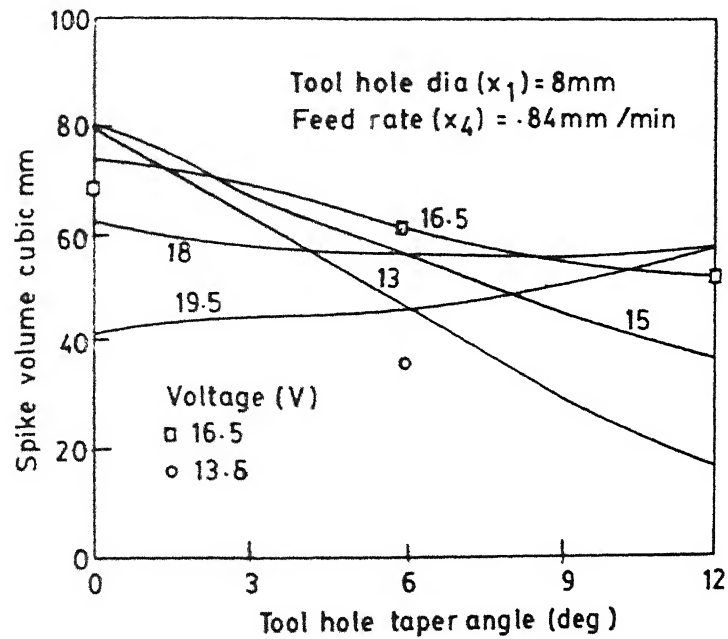
Fig. 3·12 a   Variation of spike volume with tool hole taper angle
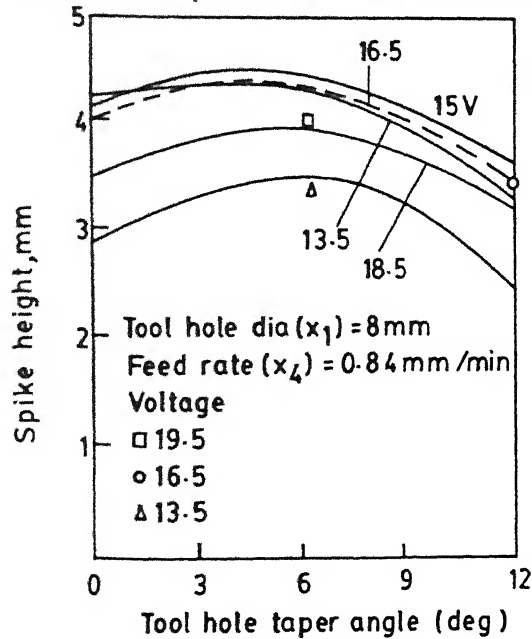
Fig. 3·12 b   Variation of spike height with tool
hole taper angle

Fig. 3.13 (a) Variation of spike volume with voltage

Tool hole dia (x_1) = 8mm
Feed rate (x_4) = 0.84 mm /min
Tool hole taper angle (x_2)
○ 6°
□ 12°

Spike volume-cubic mm
Voltage - volts
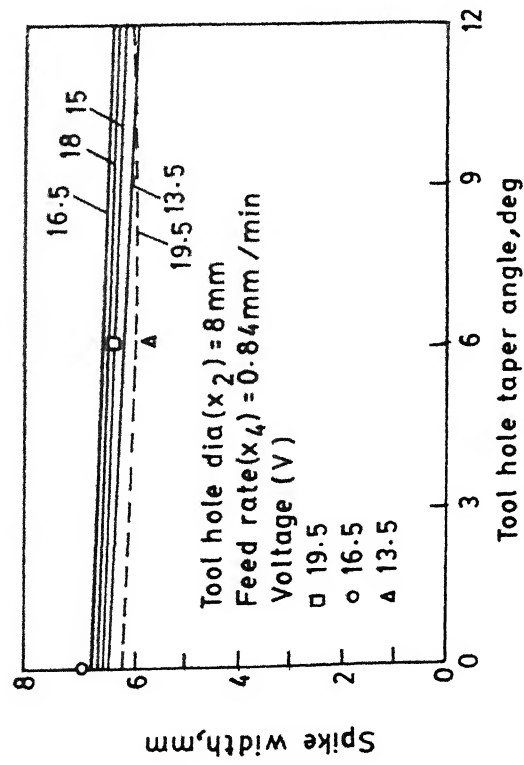
Fig. 3.12 (c) Variation of spike width with tool hole taper angle

Tool hole dia (x_2) = 8mm
Feed rate (x_4) = 0.84mm /min
Voltage (V)
□ 19.5
○ 16.5
△ 13.5

Spike width,mm
Tool hole taper angle,deg

52

Fig. 3.13 (c) Variation of spike width with voltage

Tool hole dia (x_1) = 8mm
Feed rate (x_4) = 0.84mm/min
Tool hole taper angle
□ 12°
○ 6°
▲ 0°

Fig.3.13(b) Variation of spike height with voltage

Tool hole dia (x_1) = 8mm
Feed rate = .84mm/min
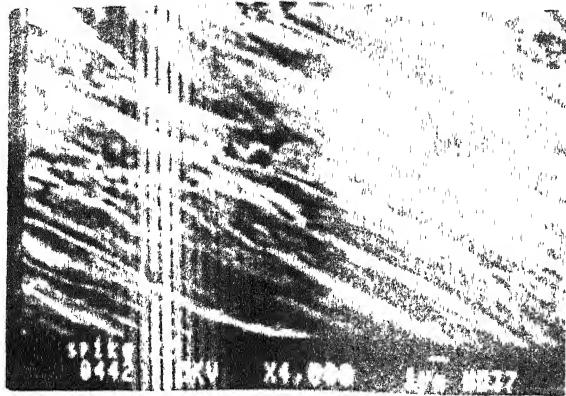Taper angle
□ 12°
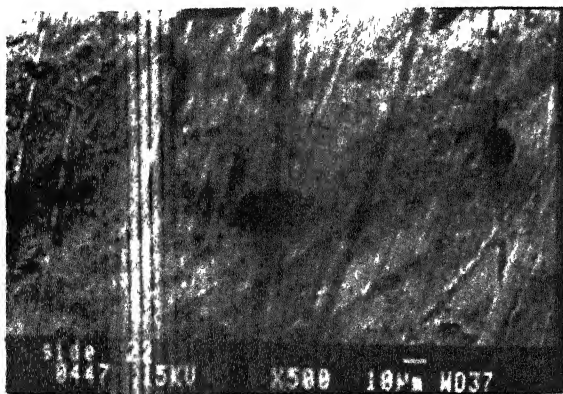○ 6°
▲ 0°
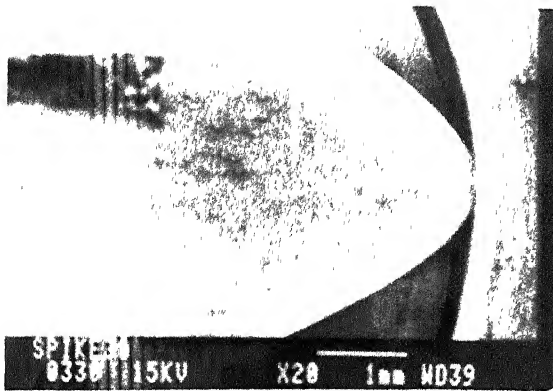
(a)
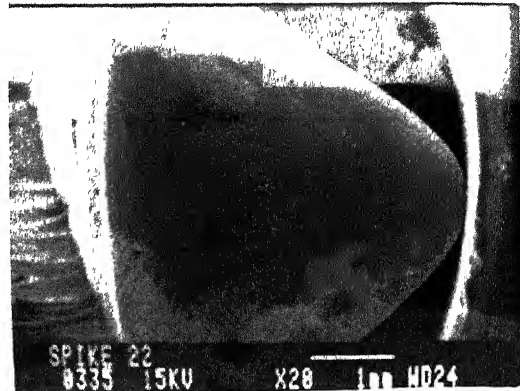
(b)
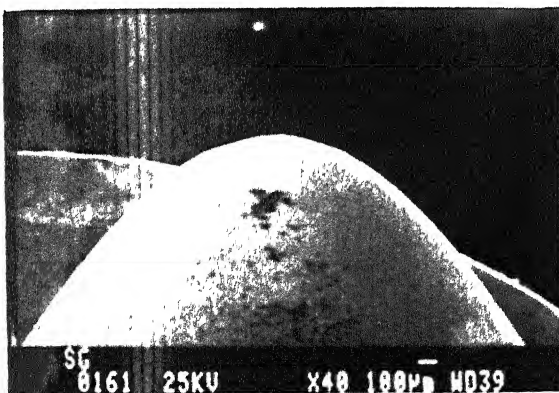
(c)
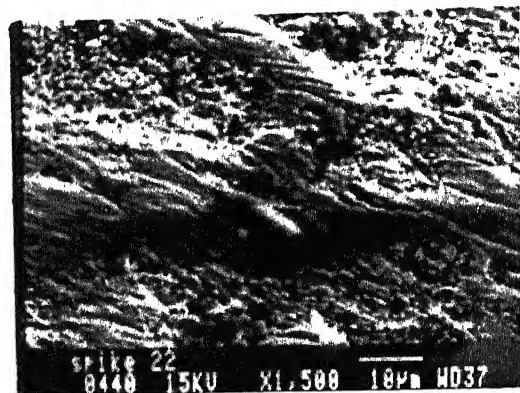
(d)

Fig. 3.14   Photograph of Surfaces by SEM

(e)

(f)

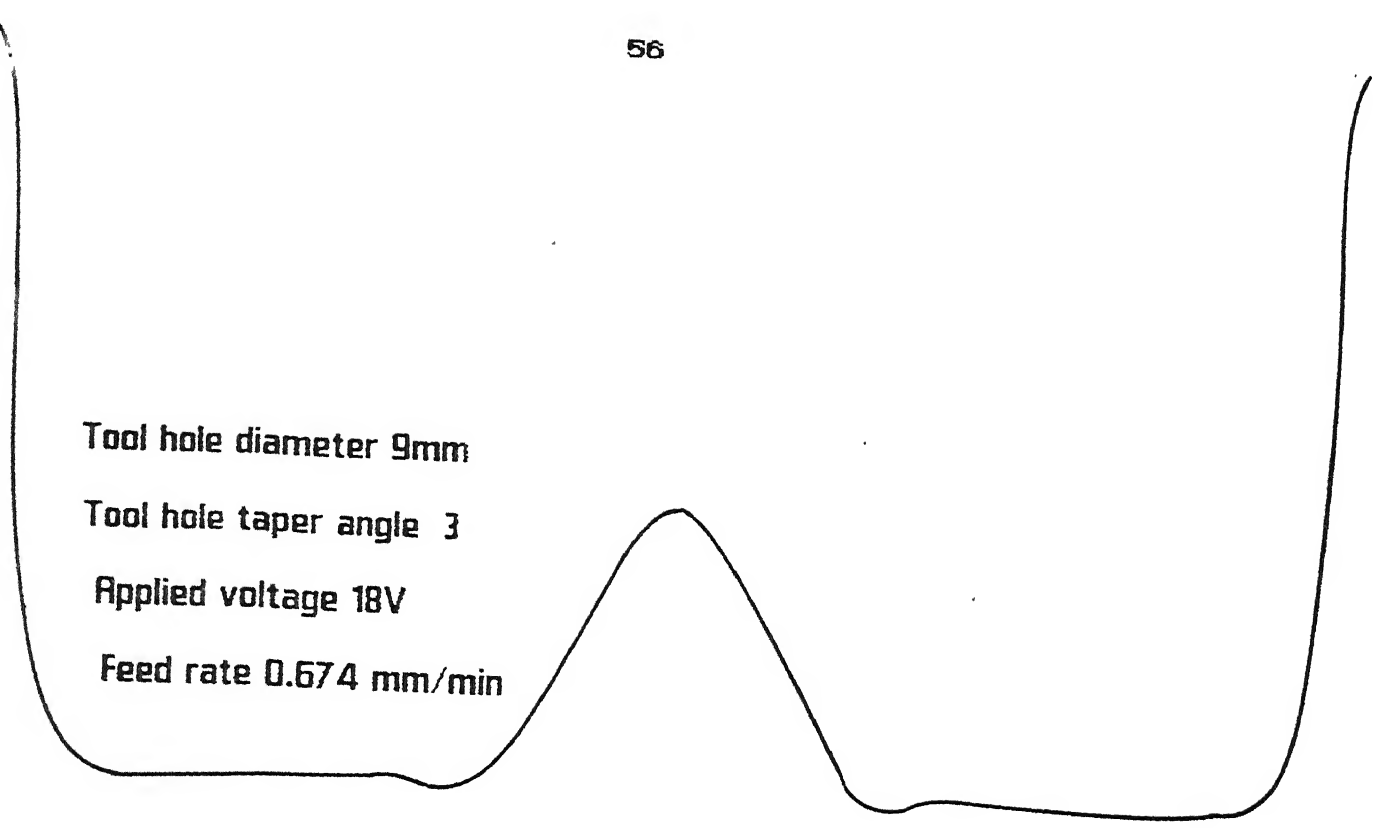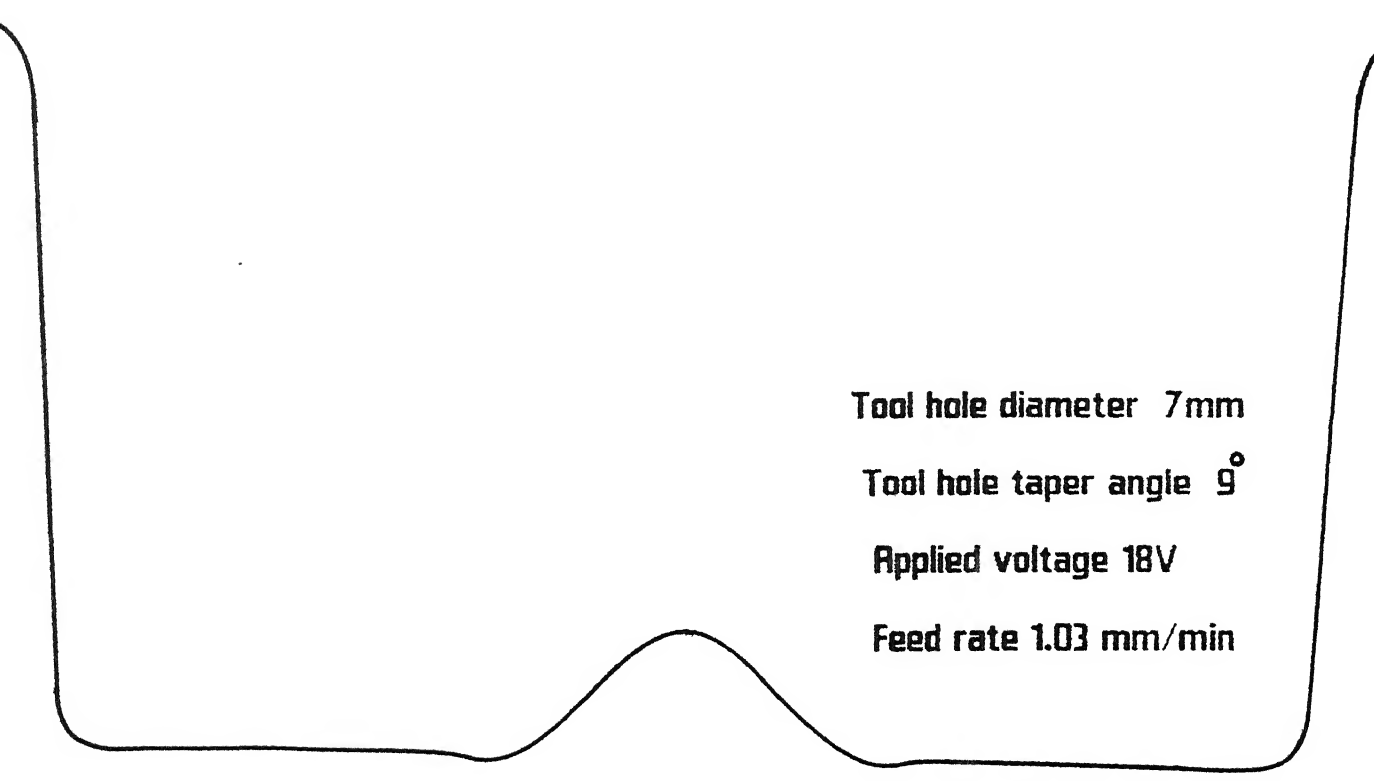
(g)
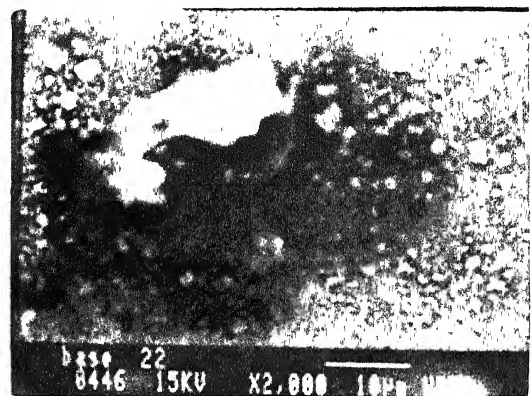
(h)

Fig. 3.14   Photograph of Surfaces by SEM

Tool hole diameter 9mm

Tool hole taper angle 3

Applied voltage 18V

Feed rate 0.674 mm/min

Fig. 3·15a(i)

Tool hole diameter 7mm
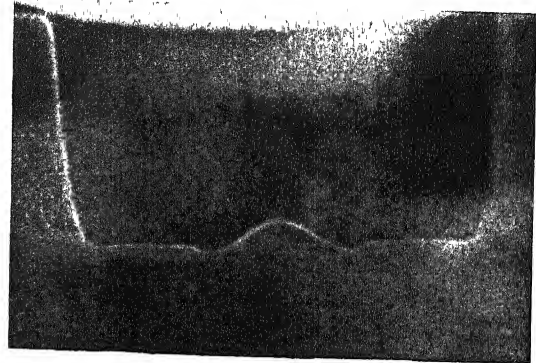
Tool hole taper angle 9°

Applied voltage 18V

Feed rate 1.03 mm/min

Fig. 3·15a(ii)

Profile of a hole by ECD [Magnification 10]
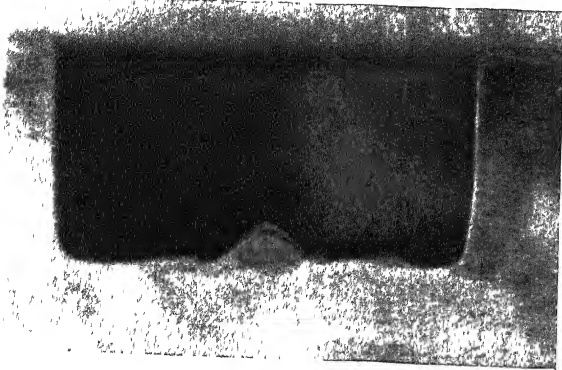
Tool hole diameter 9 mm

Tool hole taper angle , $9°$

Voltage applied 15V

Feed Rate 0.674 mm/min

Tool hole diameter 8mm

Tool hole taper angle $6°$

Voltage applied 16.5V

Feed Rate 0.5 mm/min

Fig. 3.15(b) Photograph of Electrochemically Drilled Hole

Table 3.1

Optimisation Results

			Coded Values	Actual Values
Tool hole outlet diameter	mm	X1s	-1	7
Tool hole taper angle	degree	X2s	0.6	7.48
Applied Voltage	voltage	X3s	-0.4	14.4
Feedrate	mm/min	X4s	-1.5	0.587

Table 3.2

Experiment Number	1	2	3	4
Tool hole dia (outlet) mm	10	8	8	8
Taper angle of hole (degree)	6	12	0	6
Applied Voltage V	16.5	16.5	16.5	16.5
Feed rate mm/min	0.55	1.13	0.55	1.13
Volume of Spike mm^3	80.1	94.64	34.48	114.2
Height of Spike mm	3.1	3.2	2.5	5.6
Width of Spike mm	8.6	6.8	6.1	6.9

3. The effect of other parameters like electrolyte conductivity, electrolyte composition, inter-electrode gap etc. on the characteristics of the spike can be evaluated.

4. A mathematical model would give a better insight into the underlying mechanism of the process.

5. A physiochemical study would throw light on the metallurgical aspects of the machined surface.

REFERENCES

1. Juneja, B.L. and Sekhon, G.S., "Fundamentals of Metal Cutting and Machine Tools," Wiley Eastern Ltd., New Delhi, 1987

2. Benedict, G.F.,"Non Traditional Manufacturing Processes," Marcel Dekker, Inc., New York, 1987

3. McGeough, J.A., "Advanced Methods of Machining," Chapman and Hall, London, 1988.

4. Debarr, A.E. and Oliver, D.A., "Electrochemical Machining," Macdonald and Co., Ltd.,London, 1968

5. Larsson, C.N. and Muzaffaruddin,K., "Electrochemical Effects on Shape Reproduction in ECM," 29th Int. MTDR Conf. Proceedings, 1978, pp. 533-540.

6. Kanetkar,Y., "Stray Current and Stagnation Zone Analysis in ECD During Outward Mode of Electrolyte Flow," M.Tech. Thesis, IIT Kanpur, 1987.

7. Adler Yu.P., Markava E.V., and Granousky Yn. V., "The Design of Experiments to Find Optimal Conditions," Mir Publishers, Moscow, 1975.

8. Cochran, W.G., and Cox., G.M., "Experimental Design," Asia Publishing House, 1977.

9. Bannard, J., "Fine Hole Drilling Using ECM," Proc. 19th International Machine Tool Design and Research Conference, 1980, pp. 503-510.

10.Cole, R. R. and Hopenfield, Y., "Investigations on Electrolytic Jet Polishing at High Current Densities," ASME Paper 62-WA-71,1962.

11.Loutrel,S.F. and Cook,N.H., "A Theoretical Model for High Rate ECM," Transactions of ASME, Journal of Engineering for Industry, 1973, pp. 1-6.

Appendix

```
c       program design of experiments


        double precision a(31,5),x(31,15),xt(15,31),xtx(15,15)
        double precision xtxi(15,15),xtxixt(15,31),b(15,1)
        double precision y(31,1),wkspce(31),z(1),h(31,15),c(15,31)


        open(unit=21,file='doe.in')
        open(unit=22,file='doe.out')

        read(21,*)((a(i,j),j=1,5),i=1,31)

        do 10 i=1,31
        do 10 j=1,5
        x(i,j)=a(i,j)
10      continue

        do 11 i=1,31
        x(i,6)=a(i,2)**2.
        x(i,7)=a(i,3)**2.
        x(i,8)=a(i,4)**2.
        x(i,9)=a(i,5)**2.
        x(i,10)=a(i,2)*a(i,3)
        x(i,11)=a(i,2)*a(i,4)
        x(i,12)=a(i,2)*a(i,5)
        x(i,13)=a(i,3)*a(i,4)
        x(i,14)=a(i,3)*a(i,5)
        x(i,15)=a(i,4)*a(i,5)
11      continue


        read(21,*)(y(i,1),i=1,31)


        call tpose(x,xt,31,15)
        call f01ckf(xtx,xt,x,15,15,31,z,1,1,0)
        call f01aaf(xtx,15,15,xtxi,15,wkspce,0)
        call f01ckf(xtxixt,xtxi,xt,15,31,15,z,1,1,0)
        call f01ckf(b,xtxixt,y,15,1,31,z,1,1,0)

        write(22,102)(b(i,1),i=1,15)
102     format(1(1x,f20.16))

        stop
        end


        subroutine tpose(h,c,m,n)
        double precision h(m,n),c(n,m)
        do 12 i=1,m
        do 12 j=1,n
        c(j,i)=h(i,j)
12      continue
        return
        end
```